EUROPEAN ORGANIZATION FOR NUCLEAR RESEARCH (CERN)

FERMILAB-PUB-16-106-CMS

CERN-EP/2016-043
2016/03/08

CMS-SMP-14-022

# Measurement of the differential cross section and charge asymmetry for inclusive $pp \to W^{\pm} + X$ production at $\sqrt{s} = 8\,\text{TeV}$

The CMS Collaboration*

arXiv:1603.01803v1 [hep-ex] 6 Mar 2016

## Abstract

The differential cross section and charge asymmetry for inclusive $pp \to W^{\pm} + X \to \mu^{\pm}\nu + X$ production at $\sqrt{s} = 8\,\text{TeV}$ are measured as a function of muon pseudorapidity. The data sample corresponds to an integrated luminosity of $18.8\,\text{fb}^{-1}$ recorded with the CMS detector at the LHC. These results provide important constraints on the parton distribution functions of the proton in the range of the Bjorken scaling variable $x$ from $10^{-3}$ to $10^{-1}$.

*Submitted to the European Physical Journal C*

© 2016 CERN for the benefit of the CMS Collaboration. CC-BY-3.0 license

*See Appendix A for the list of collaboration members

Operated by Fermi Research Alliance, LLC under Contract No. De-AC02-07CH11359 with the United States Department of Energy.

# 1 Introduction

We present measurements of the $\mathrm{pp} \to \mathrm{W}^{\pm} + \mathrm{X} \to \mu^{\pm}\nu + \mathrm{X}$ differential cross section and the muon charge asymmetry that provide important constraints on the valence and sea quark distributions in the proton. Uncertainties in the parton distribution functions (PDF) have become a limiting factor for the precision of many inclusive and differential cross section calculations, given the development of precise theoretical tools describing hard scattering processes in pp collisions.

For each charge of the W boson, the differential cross section,

$$\sigma_{\eta}^{\pm} = \frac{\mathrm{d}\sigma}{\mathrm{d}\eta}(\mathrm{pp} \to \mathrm{W}^{\pm} + \mathrm{X} \to \mu^{\pm}\nu + \mathrm{X}), \tag{1}$$

is measured in bins of muon pseudorapidity $\eta = -\ln\tan(\theta/2)$ in the laboratory frame, where $\theta$ is the polar angle of the muon direction with respect to the beam axis. Current theoretical calculations predict these cross sections with next-to-next-to-leading-order (NNLO) accuracy in perturbative quantum chromodynamics (QCD). The dominant $\mathrm{W}^{\pm}$ boson production occurs through the annihilation of a valence quark from one of the protons with a sea antiquark from the other: $\mathrm{u}\overline{\mathrm{d}} \to \mathrm{W}^{+}$ and $\mathrm{d}\overline{\mathrm{u}} \to \mathrm{W}^{-}$. Because of the presence of two valence u quarks in the proton, $\mathrm{W}^{+}$ bosons are produced more often than $\mathrm{W}^{-}$ bosons. Precise measurement of the charge asymmetry as a function of the muon $\eta$,

$$\mathcal{A}(\eta) = \frac{\sigma_{\eta}^{+} - \sigma_{\eta}^{-}}{\sigma_{\eta}^{+} + \sigma_{\eta}^{-}}, \tag{2}$$

provides significant constraints on the ratio of u and d quark distributions in the proton for values of $x$, the Bjorken scaling variable [1], between $10^{-3}$ and $10^{-1}$.

The $\mathrm{W}^{\pm}$ boson production asymmetry was previously studied in $\mathrm{p}\overline{\mathrm{p}}$ collisions by the CDF and D0 collaborations [2–6]. At the LHC, the first measurements of the lepton charge asymmetries were performed by the CMS, ATLAS, and LHCb experiments using data collected in 2010 [7–9]. The CMS experiment has further improved the measurement precision in both the electron and muon decay channels using data from pp collisions at $\sqrt{s} = 7\,\mathrm{TeV}$ corresponding to integrated luminosities of $0.84\,\mathrm{fb}^{-1}$ and $4.7\,\mathrm{fb}^{-1}$ in the electron [10] and muon [11] decay channels, respectively.

This measurement is based on a data sample of pp collisions at $\sqrt{s} = 8\,\mathrm{TeV}$ collected by CMS during 2012, corresponding to an integrated luminosity of $18.8\,\mathrm{fb}^{-1}$. At $\sqrt{s} = 8\,\mathrm{TeV}$ the average value of the Bjorken scaling variable for the interacting partons in $\mathrm{W}^{\pm}$ boson production is lower than at $\sqrt{s} = 7\,\mathrm{TeV}$, which is expected to result in a lower $\mathrm{W}^{\pm}$ boson production charge asymmetry. This measurement provides important constraints on the proton PDFs, which is illustrated by the QCD analysis also presented in this paper.

# 2 CMS detector

The central feature of the CMS apparatus is a superconducting solenoid of 6 m internal diameter, providing a magnetic field of 3.8 T. Within the solenoid volume are a silicon pixel and strip tracker, a lead tungstate crystal electromagnetic calorimeter, and a brass and scintillator hadron calorimeter, each composed of a barrel and two endcap sections. Muons are measured in gas-ionization detectors embedded in the steel flux-return yoke outside the solenoid. Extensive forward calorimetry complements the coverage provided by the barrel and endcap detectors.

A more detailed description of the CMS detector, together with a definition of the coordinate system used and the relevant kinematic variables, can be found in Ref. [12].

# 3 Data selection and simulation

A $W^{\pm} \to \mu^{\pm}\nu$ event is characterized by an isolated muon with a high transverse momentum $p_T$ and a large missing transverse energy $\not{E}_T$ associated with an undetected neutrino. Events in this sample are collected with an isolated single-muon trigger with a $p_T$ threshold of 24 GeV. To reduce the background, identification and isolation criteria are applied to the reconstructed muons. These requirements are similar to those used in the previous measurement [11]. Muon tracks must be reconstructed in both the silicon tracker and the muon detectors. The global muon fit is required to have a $\chi^2$ per degree of freedom less than 10. The pseudorapidity coverage for reconstructed muons is restricted to $|\eta| < 2.4$. Cosmic ray contamination is largely reduced by rejecting the muon candidates with a large ($>$0.2 cm) distance of closest approach to the primary vertex in the transverse plane. The isolation criterion is based on additional tracks reconstructed in a cone of $\sqrt{(\Delta\eta)^2 + (\Delta\phi)^2} < 0.3$ around the muon, where $\phi$ is the azimuthal angle (in radians) in the laboratory frame. The muon candidate is rejected if the scalar $p_T$ sum of these tracks is more than 10% of the muon $p_T$. The selected muon candidate with the largest $p_T$, identified as a signal muon from the W boson decay, is required to have a $p_T > 25$ GeV and also to be the particle that triggered the event. To reduce the background from Drell–Yan (DY) dimuon production, events containing a second identified muon with $p_T > 15$ GeV are rejected.

A total of about 61 million $W^+ \to \mu^+\nu$ and 45 million $W^- \to \mu^-\bar{\nu}$ candidate events are selected. The $W^{\pm} \to \mu^{\pm}\nu$ signal is contaminated with backgrounds that also produce a muon with high $p_T$. The major background sources are (i) multijet (QCD) events with high-$p_T$ muons produced in hadron decays (about 10% of the selected sample), and (ii) $Z/\gamma^* \to \mu^+\mu^-$ events (5% of the sample). The contribution from other backgrounds, such as $W^{\pm} \to \tau^{\pm}\nu$ (2.6%), $Z/\gamma^* \to \tau^+\tau^-$ (0.5%), and $t\bar{t}$ (0.5%) events, is relatively small. The contributions from single top quark (0.14%) and diboson (0.07%) events, as well as from cosmic muons ($10^{-5}$), are negligible.

Simulated samples are used to model the signal and background processes. The signal, as well as the electroweak and $t\bar{t}$ background samples, is based on the next-to-leading-order (NLO) matrix element calculations implemented in the POWHEG Monte Carlo (MC) event generator [13–16], interfaced with PYTHIA6 [17] for parton showering and hadronization, including electromagnetic final-state radiation (FSR). The CT10 NLO PDFs [18] are used. The $\tau$ lepton decays in relevant processes are simulated with TAUOLA [19].

The QCD background is generated with PYTHIA6 using CTEQ6L PDF [20]. The detector response to all generated particles is simulated with GEANT4 [21]. Final-state particles are reconstructed with the same algorithms used for the data sample. To match the distribution of the number of additional interactions per bunch crossing (pileup) observed in data, weight factors are applied to all simulated events in signal and background samples. The weight factors are based on the instantaneous luminosity and the total inelastic cross section of 69.4 mb measured by CMS [22].

# 4 Corrections to the data and simulations

The fiducial cross sections are measured for muon $p_T > 25$ GeV in 11 bins of absolute pseudorapidity, covering the range $|\eta| < 2.4$. The $|\eta|$ binning is such that the migration effects

due to the finite $\eta$ resolution are negligible. In each $|\eta|$ bin, the number of $W^+ \to \mu^+\nu$ and $W^- \to \mu^-\nu$ events is extracted by fitting the $\not{E}_T$ distributions with signal and background distributions (templates). The template shapes and initial normalizations are derived from MC simulations. To improve the simulation, several corrections are applied to the MC samples. The corrections, which are similar to those used in the previous measurement [11], are briefly summarized below.

Accurate calibration of the muon momentum is important for the proper modeling of the yields of $W^\pm$ events and of the shapes of $\not{E}_T$ templates. Dominant sources of the muon momentum mismeasurement are the mismodeling of the tracker alignment and the magnetic field. Muon momentum correction factors are derived using $Z/\gamma^* \to \mu^+\mu^-$ events in several iterations [23]. First, "reference" distributions are defined based on the MC generated muons, with momenta smeared by the reconstruction resolution. Then, corrections to muon momentum in bins of $\eta$ and $\phi$ are extracted separately for positively and negatively charged muons. These corrections match the mean values of reconstructed $1/p_T$ spectra to the corresponding reference values. Finally, correction factors are tuned further by comparing the reconstructed dimuon invariant mass spectra in each $\mu^+$ and $\mu^-$ pseudorapidity bin with the reference. The correction factors are determined separately for data and simulated events following the same procedure.

The overall muon selection efficiency includes contributions from reconstruction, identification, isolation, and trigger efficiencies. Each component is measured from $Z/\gamma^* \to \mu^+\mu^-$ events using the "tag-and-probe" method [24, 25]. The efficiencies are measured in bins of $\eta$ and $p_T$ for $\mu^+$ and $\mu^-$ separately. Each $\eta$ bin of the efficiency measurement is fully contained in a single $|\eta|$ bin used for the asymmetry measurement. The total average efficiency is about 85% at central rapidities and drops to about 50% in the last $|\eta|$ bin. The ratio of the average $\mu^+$ and $\mu^-$ efficiencies varies within 0.6% of unity in the first 10 $|\eta|$ bins. In the last bin the ratio is 0.98. The same procedure is used in data and MC simulation, and scale factors are determined to match the MC simulation efficiencies to data.

Template shapes, used in the fits, are based on the missing transverse momentum ($\vec{p}_T^{\,miss}$) reconstructed with the particle-flow algorithm [26, 27]. The $\vec{p}_T^{\,miss}$ is defined as the projection on the plane perpendicular to the beams of the negative vector sum of the momenta of all reconstructed particles in an event. A set of corrections is applied to $\vec{p}_T^{\,miss}$ in order to improve the modeling of distributions of $\not{E}_T = |\vec{p}_T^{\,miss}|$ in data and MC templates. First, the average bias in the $\vec{p}_T^{\,miss}$-component along the direction of $\vec{p}_T$-sum of charged particles associated with the pileup vertices is removed [28]. Second, the muon momentum correction to $\vec{p}_T$, described above, is added vectorially to $\vec{p}_T^{\,miss}$. In addition, the "$\phi$-modulation" corrections, which increase linearly as a function of pileup, make the $\phi(\vec{p}_T^{\,miss})$ distributions uniform [28]. The above corrections are applied to both data and simulated events. The final set of corrections, derived from the "hadronic recoil" technique [29, 30], is applied to simulated $W^\pm \to \mu^\pm\nu$, $Z/\gamma^* \to \mu^+\mu^-$, and QCD events to match the average $\vec{p}_T^{\,miss}$ scale and resolution to data.

The modeling of the multijet events is further improved with a set of corrections derived from a QCD control sample selected by inverting the offline isolation requirement for events collected using a prescaled muon trigger with no isolation requirement. Muon $p_T$-dependent weight factors are determined for the QCD simulation that match the muon $p_T$ distributions with data.

## 5 Signal extraction

In each of the 11 muon $|\eta|$ bins, yields of $W^+$ and $W^-$ events are obtained from the simultaneous $\chi^2$-fit of the $\not{E}_T$ distributions of $\mu^+$ and $\mu^-$ events. The definition of $\chi^2$ used in the fit

takes into account the statistical uncertainties in the simulated templates. The shapes of the $\not{E}_T$ distributions for the $W^{\pm} \to \mu^{\pm}\nu$ signal and the backgrounds are taken from the MC simulation after correcting for mismodeling of the detector response and for the $p_T$ distribution of W bosons. All electroweak and $t\bar{t}$ background samples are normalized to the integrated luminosity using the theoretical cross sections calculated at NNLO. Each simulated event is also weighted with scale factors to match the average muon selection efficiencies in data. In addition, mass-dependent correction factors are applied to $Z/\gamma^* \to \mu^+\mu^-$ simulated events to match the observed mass distribution of dimuon events in data.

The $W^+$ and $W^-$ signal yields and QCD background normalization are free parameters in the fit. The relative contributions of QCD background events in the $W^+$ and $W^-$ samples are constrained to values obtained from the QCD control sample. The $W^{\pm} \to \tau^{\pm}\nu$ background is normalized to the $W^{\pm} \to \mu^{\pm}\nu$ signal, for each charge, using the scale factors corresponding to the free parameters of the signal yield. The normalizations of the remaining electroweak and $t\bar{t}$ backgrounds are fixed in the fit.

Table 1 summarizes the fitted yields of $W^+$ ($N^+$) and $W^-$ ($N^-$) events, the correlation coefficient ($\rho_{+,-}$), and the $\chi^2$ value for each fit. Examples of fits for three $|\eta|$ ranges are shown in Fig. 1. The ratio of the data to the final fit, shown below each distribution, demonstrates good agreement of the fits with data.

Table 1: Summary of the fitted $N^+$, $N^-$, the correlation ($\rho_{+,-}$) between the uncertainties in $N^+$ and $N^-$, and the $\chi^2$ of the fit for each $|\eta|$ bin. The number of degrees of freedom ($n_{\text{dof}}$) in each fit is 197. The quoted uncertainties are statistical. The correlation coefficients are expressed as percentages.

| $\|\eta\|$ bin | $\chi^2$ ($n_{\text{dof}}$ = 197) | $N^+$ ($10^3$) | $N^-$ ($10^3$) | $\rho_{+,-}$ (%) |
|---|---|---|---|---|
| 0.00–0.20 | 238 | $4648.5 \pm 4.2$ | $3584.9 \pm 3.8$ | 18.9 |
| 0.20–0.40 | 242 | $4414.5 \pm 4.0$ | $3360.9 \pm 3.7$ | 18.8 |
| 0.40–0.60 | 248 | $4893.8 \pm 4.3$ | $3692.5 \pm 3.9$ | 18.9 |
| 0.60–0.80 | 199 | $4900.1 \pm 4.3$ | $3621.3 \pm 3.8$ | 19.2 |
| 0.80–1.00 | 218 | $4420.8 \pm 4.0$ | $3218.0 \pm 3.6$ | 18.7 |
| 1.00–1.20 | 204 | $4235.7 \pm 3.9$ | $2949.2 \pm 3.4$ | 18.5 |
| 1.20–1.40 | 193 | $4176.8 \pm 3.9$ | $2827.0 \pm 3.5$ | 19.3 |
| 1.40–1.60 | 213 | $4351.2 \pm 4.2$ | $2864.7 \pm 3.7$ | 19.3 |
| 1.60–1.85 | 208 | $4956.2 \pm 4.4$ | $3134.1 \pm 3.9$ | 19.5 |
| 1.85–2.10 | 238 | $5292.9 \pm 4.4$ | $3229.6 \pm 3.8$ | 18.5 |
| 2.10–2.40 | 229 | $4023.7 \pm 3.9$ | $2428.2 \pm 3.3$ | 17.6 |

For each muon charge and $|\eta|$ bin, the fiducial cross section is calculated as

$$\sigma_{\eta}^{\pm} = \frac{1}{2\Delta\eta} \frac{N^{\pm}}{\epsilon^{\pm}\epsilon_{\text{FSR}}^{\pm}\mathcal{L}_{\text{int}}}, \tag{3}$$

where $\epsilon^{\pm}$ is the average $\mu^{\pm}$ selection efficiency per $|\eta|$ bin, $\epsilon_{\text{FSR}}$ takes into account the event loss within the muon $p_T$ acceptance due to the final-state photon emission, and $\mathcal{L}_{\text{int}}$ is the integrated luminosity of the data sample. The calculation of the average $\epsilon^{\pm}$ in each bin is based on the scale factors, measured from $Z/\gamma^* \to \mu^+\mu^-$ events for each charge, that match the muon selection efficiencies of simulation and data. Each $\epsilon_{\text{FSR}}^{\pm}$ factor, defined as a ratio of the numbers of events within the $p_T$ acceptance after and before FSR, is evaluated using the signal MC samples.

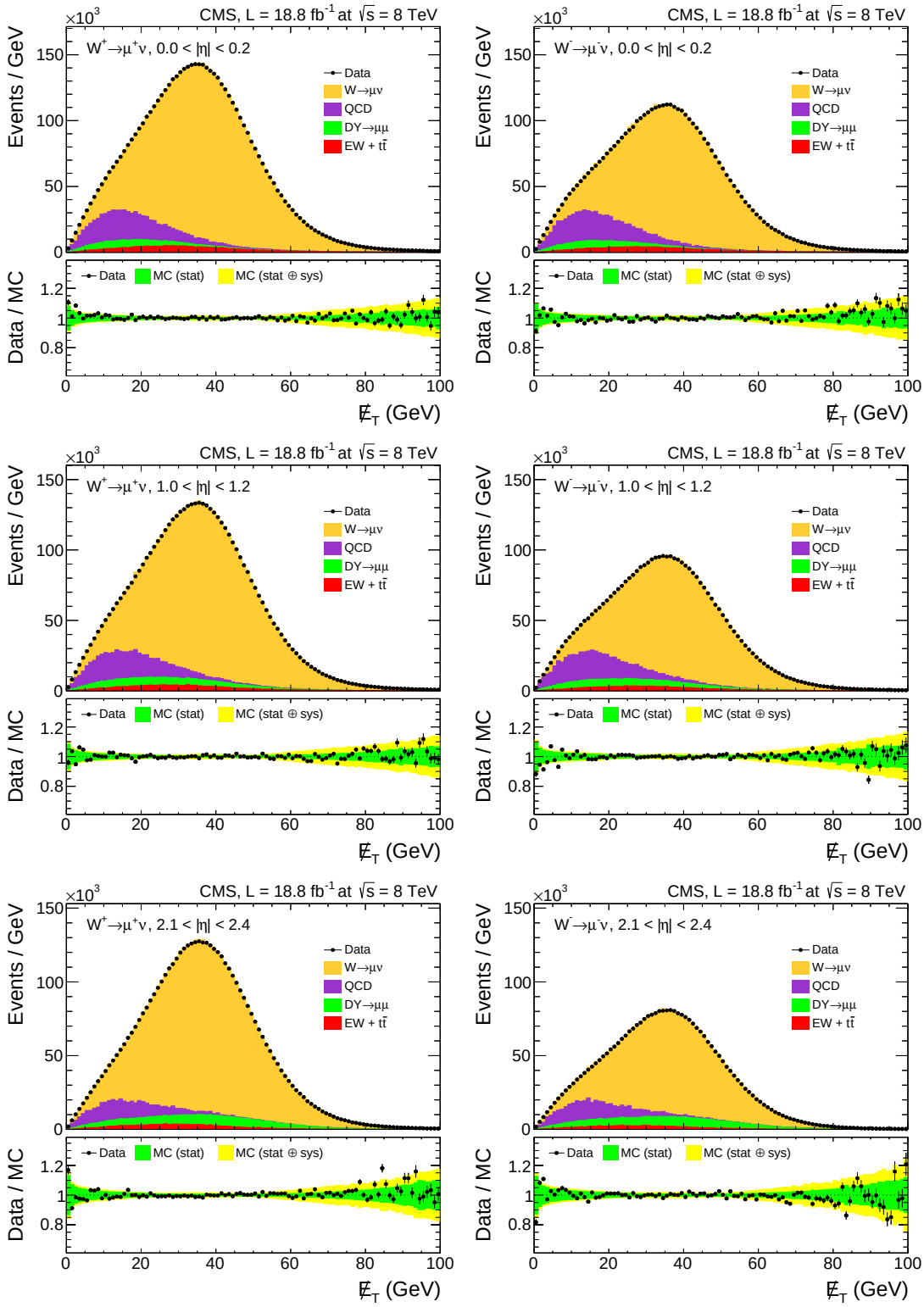


Figure 1: Examples of fits in three $|\eta|$ ranges: $0.0 < |\eta| < 0.2$ (top), $1.0 < |\eta| < 1.2$ (center), and $2.1 < |\eta| < 2.4$ (bottom). For each $\eta$ range, results for $W^+$ (left) and $W^-$ (right) are shown. The ratios between the data points and the final fits are shown at the bottom of each panel.

# 6 Systematic uncertainties

To estimate the systematic uncertainties in the muon selection efficiencies, several variations are applied to the measured efficiency tables. First, the efficiency values in each $\eta$–$p_{\mathrm{T}}$ bin are varied within their statistical errors for data and simulation independently. In each pseudo-experiment the varied set of efficiencies is used to correct the MC simulation templates and extract the cross sections using Eq. (3). The standard deviation of the resulting distribution is taken as a systematic uncertainty for each charge and $|\eta|$ bin. The statistical uncertainties between the two charges and all $\eta$–$p_{\mathrm{T}}$ bins are uncorrelated. Second, the offline muon selection efficiency scale factors are varied by $\pm 0.5\%$ coherently for both charges and all bins. The trigger selection efficiency scale factors are varied by $\pm 0.2\%$, assuming no correlations between the $\eta$ bins, but $+100\%$ correlations between the charges and $p_{\mathrm{T}}$ bins. The above systematic variations take into account uncertainties associated with the tag-and-probe technique and are assessed by varying signal and background dimuon mass shapes, levels of background, and dimuon mass range and binning used in the fits. Finally, an additional $\pm 100\%$ correlated variation is applied based on the bin-by-bin difference between the true and measured efficiencies in the $\mathrm{Z}/\gamma^* \to \mu^+\mu^-$ MC sample. This difference changes gradually from about 0.5% in the first bin to about $-2\%$ in the last bin. This contribution is the main source of negative correlations in the systematic uncertainties between the central and high rapidity bins. The total systematic uncertainty in the efficiency is obtained by adding up the four covariance matrices corresponding to the above variations.

A possible mismeasurement of the charge of the muon could lead to a bias in the observed asymmetry between the $\mathrm{W}^+$ and $\mathrm{W}^-$ event rates. The muon charge misidentification rate has been studied in detail and was found to be negligible ($10^{-5}$) [7].

The muon momentum correction affects the yields and the shapes of the $\not{E}_{\mathrm{T}}$ distributions in both data and MC simulation. To estimate the systematic uncertainty, the muon correction parameters in each $\eta$–$\phi$ bin and overall scale are varied within their uncertainties. The standard deviation of the resulting cross section distribution for each charge and muon $|\eta|$ bin is taken as the systematic uncertainty and the corresponding correlations are calculated. Finite detector resolution effects, which result in the migration of events around the $p_{\mathrm{T}}$ threshold and between $|\eta|$ bins, have been studied with the signal MC sample and found to have a negligible impact on the measured cross sections and asymmetries.

There are two sources of systematic uncertainties associated with the QCD background estimate. One is the uncertainty in the ratio of QCD background events in the $\mathrm{W}^+$ and $\mathrm{W}^-$ samples ($R_{\pm}^{\mathrm{QCD}}$). Whereas the total QCD normalization is one of the free parameters in the fit, $R_{\pm}^{\mathrm{QCD}}$is constrained to the value observed in the QCD control sample, which varies within 3% of unity depending on the $|\eta|$ bin. The corresponding systematic uncertainty is evaluated by changing it by $\pm 5\%$ in each $|\eta|$ bin. This variation covers the maximum deviations indicated by the QCD MC simulation. The resulting systematic uncertainties are assumed to be uncorrelated between the $|\eta|$ bins. Additionally, the average difference of this ratio between the signal and QCD control regions is evaluated using the QCD MC simulation. This difference of about 3% is taken as an additional 100%-correlated systematic uncertainty in $R_{\pm}^{\mathrm{QCD}}$. As a check, using the same shape for the QCD background in $\mu^+$ and $\mu^-$ events, its normalization is allowed to float independently for the two charges. The resulting values of $R_{\pm}^{\mathrm{QCD}}$are covered by the above systematic uncertainties.

The other component of systematic uncertainty, associated with the QCD background, is the $\not{E}_{\mathrm{T}}$ shape. To estimate the systematic uncertainty in modeling the shape of the $\not{E}_{\mathrm{T}}$ distributions

in QCD events, additional fits are performed using the $\not{E}_T$ distributions without the hadronic recoil corrections and the $p_T$-dependent scale factors; this results in a variation of about 2% in the average $\not{E}_T$ resolution. The resulting shifts in the extracted cross section values in each $|\eta|$ bin are taken as systematic uncertainties. The correlations between the $|\eta|$ bins and the two charges are assumed to be 100%.

The normalization of the $Z/\gamma^* \to \mu^+\mu^-$ background in the signal region is corrected with mass-dependent scale factors that match the dimuon mass distribution in MC simulation with data. The systematic uncertainty is the difference between the cross sections calculated with and without applying these corrections to the DY background normalizations. An uncertainty of 7% is assigned to the $t\bar{t}$ theoretical cross section [31], which is used to normalize the $t\bar{t}$ background to the integrated luminosity of the data sample. In the fits, the $W^\pm \to \tau^\pm\nu$ background is normalized to the $W^\pm \to \mu^\pm\nu$ yields in data with a ratio obtained from the simulation. A $\pm 2\%$ uncertainty is assigned to the $W^\pm \to \tau^\pm\nu$ to $W^\pm \to \mu^\pm\nu$ ratio [32]. Each of the above variations is assumed to be fully correlated for the different bins and the two charges.

There are several sources of systematic uncertainty that affect the $\not{E}_T$ shapes. The systematic uncertainty associated with the $\phi$ modulation of $\vec{p}_T^{\,miss}$ is small and is evaluated by removing the corresponding correction to $\vec{p}_T^{\,miss}$. The effect of mismodeling the pileup in the simulation is estimated by varying the minimum bias cross section by 5% and reweighting the MC events to match the expected pileup distributions in data. To improve the agreement between data and simulation, the W boson $p_T$ spectrum is weighted using factors determined by the ratios of the $p_T$ distributions in $Z/\gamma^* \to \mu^+\mu^-$ events in data and MC simulation. The difference in measured cross sections with and without this correction is taken as a systematic uncertainty. Each of the sources above are assumed to be fully correlated between the two charges and different bins. Systematic uncertainties associated with the recoil corrections are evaluated by varying the average recoil and resolution parameters within their uncertainties. The standard deviation of the resulting cross section distribution is taken as the systematic uncertainty and correlations between the two charges and different bins are calculated.

The emission of FSR photons tends, on average, to reduce the muon $p_T$. The observed post-FSR cross sections within the $p_T$ acceptance are corrected using the $\epsilon^\pm_{FSR}$ factors derived from the signal MC sample. The difference between the $p_T$ spectra of positive and negative muons results in smaller charge asymmetries after FSR compared with those before FSR within the same $p_T > 25\,\text{GeV}$ acceptance. These differences, which vary between 0.07% and 0.11% depending on the $|\eta|$ bin, are corrected by the charge-dependent $\epsilon^\pm_{FSR}$ efficiency factors. The systematic uncertainty in the FSR modeling is estimated by reweighting events with radiated photons with correction factors that account for missing electroweak corrections in the parton shower [33, 34]. The $\epsilon^\pm_{FSR}$ correction factors are reevaluated after such reweighting, and the difference between the cross sections, calculated with the new and default $\epsilon^\pm_{FSR}$ values, is taken as a systematic uncertainty. The correlations between the two charges and different $|\eta|$ bins are assumed to be 100%. The effects of migration between the $|\eta|$ bins due to final-state photon emission have been evaluated with the signal MC sample and are found to be negligible.

The PDF uncertainties are evaluated by using the NLO MSTW2008 [35], CT10 [18], and NNPDF2.1 [36] PDF sets. All simulated events are weighted according to a given PDF set, varying both the template normalizations and shapes. For CT10 and MSTW2008 PDFs, asymmetric master equations are used [18, 35]. For the NNPDF2.1 PDF set, the standard deviation of the extracted cross section distributions is taken as a systematic uncertainty. For the CT10, the 90% confidence level (CL) uncertainty is rescaled to 68% CL using a factor of 1.645. The half-width of the total envelope of all three PDF uncertainty bands is taken as the PDF uncertainty. The

Table 2: Systematic uncertainties in cross sections ($\delta\sigma_\eta^\pm$) and charge asymmetry ($\delta\mathcal{A}$) for each $|\eta|$ bin. The statistical and integrated luminosity uncertainties are also shown for comparison. A detailed description of each systematic uncertainty is given in the text.

| $\lvert\eta\rvert$ bin | 0.0–0.2 | 0.2–0.4 | 0.4–0.6 | 0.6–0.8 | 0.8–1.0 | 1.0–1.2 | 1.2–1.4 | 1.4–1.6 | 1.6–1.85 | 1.85–2.1 | 2.1–2.4 |
|---|---|---|---|---|---|---|---|---|---|---|---|
| | | | | | $\delta\sigma_\eta^+$ (pb) | | | | | | |
| Efficiency | 5.5 | 7.0 | 6.3 | 6.2 | 6.6 | 4.5 | 4.3 | 4.3 | 5.3 | 6.9 | 17.7 |
| Muon scale | 0.4 | 0.4 | 0.4 | 0.4 | 0.4 | 0.5 | 0.5 | 0.5 | 0.5 | 0.5 | 0.4 |
| QCD $+/-$ | 1.1 | 1.1 | 1.1 | 1.1 | 1.1 | 1.1 | 1.2 | 1.3 | 1.2 | 1.0 | 0.7 |
| QCD shape | 2.0 | 1.9 | 2.0 | 2.0 | 1.9 | 1.9 | 2.0 | 2.3 | 2.1 | 1.5 | 1.0 |
| EW+$t\bar{t}$ bkg | 0.6 | 0.6 | 0.6 | 0.6 | 0.6 | 0.7 | 0.8 | 0.9 | 1.0 | 1.2 | 1.3 |
| $\not{E}_T$ shape | 2.4 | 2.4 | 2.5 | 2.4 | 2.4 | 2.5 | 2.8 | 2.9 | 2.9 | 2.4 | 1.9 |
| PDF | 0.6 | 0.5 | 0.5 | 0.5 | 0.7 | 0.9 | 1.1 | 1.3 | 1.6 | 1.8 | 2.0 |
| FSR | 0.2 | 0.2 | 0.2 | 0.2 | 0.2 | 0.2 | 0.2 | 0.1 | 0.1 | 0.0 | 0.0 |
| Total syst. | 6.5 | 7.7 | 7.2 | 7.1 | 7.4 | 5.8 | 5.8 | 6.1 | 6.8 | 7.9 | 18.0 |
| Int. lum. | 19.3 | 19.5 | 19.5 | 19.6 | 19.8 | 19.9 | 20.1 | 20.1 | 20.2 | 20.0 | 19.5 |
| Stat. | 0.7 | 0.7 | 0.7 | 0.7 | 0.7 | 0.7 | 0.7 | 0.7 | 0.7 | 0.6 | 0.7 |
| Total unc. | 20.4 | 21.0 | 20.8 | 20.9 | 21.2 | 20.7 | 21.0 | 21.0 | 21.3 | 21.6 | 26.5 |
| | | | | | $\delta\sigma_\eta^-$ (pb) | | | | | | |
| Efficiency | 4.3 | 5.5 | 4.8 | 4.6 | 4.4 | 3.2 | 2.9 | 2.8 | 3.4 | 4.0 | 10.1 |
| Muon scale | 0.3 | 0.3 | 0.3 | 0.3 | 0.3 | 0.3 | 0.3 | 0.4 | 0.4 | 0.3 | 0.3 |
| QCD $+/-$ | 0.9 | 0.9 | 0.9 | 0.9 | 0.9 | 0.9 | 1.0 | 1.0 | 1.0 | 0.8 | 0.5 |
| QCD shape | 1.8 | 1.8 | 1.9 | 1.8 | 1.8 | 1.8 | 2.0 | 2.1 | 2.1 | 1.5 | 1.0 |
| EW+$t\bar{t}$ bkg | 0.5 | 0.5 | 0.5 | 0.6 | 0.6 | 0.6 | 0.7 | 0.8 | 0.9 | 1.1 | 1.2 |
| $\not{E}_T$ shape | 2.2 | 2.2 | 2.3 | 2.2 | 2.3 | 2.4 | 2.5 | 2.8 | 2.7 | 2.3 | 1.7 |
| PDF | 0.6 | 0.6 | 0.5 | 0.5 | 0.7 | 0.8 | 1.1 | 1.2 | 1.5 | 1.6 | 1.9 |
| FSR | 0.2 | 0.2 | 0.1 | 0.1 | 0.1 | 0.1 | 0.1 | 0.1 | 0.1 | 0.1 | 0.1 |
| Total syst. | 5.3 | 6.4 | 5.7 | 5.5 | 5.5 | 4.6 | 4.6 | 4.9 | 5.2 | 5.3 | 10.6 |
| Int. lum. | 14.8 | 14.8 | 14.7 | 14.5 | 14.3 | 13.9 | 13.6 | 13.2 | 12.7 | 12.1 | 11.4 |
| Stat. | 0.6 | 0.6 | 0.6 | 0.6 | 0.6 | 0.6 | 0.6 | 0.6 | 0.6 | 0.6 | 0.6 |
| Total unc. | 15.7 | 16.1 | 15.8 | 15.5 | 15.3 | 14.7 | 14.3 | 14.1 | 13.7 | 13.2 | 15.6 |
| | | | | | $\delta\mathcal{A} \times 100$ | | | | | | |
| Efficiency | 0.06 | 0.07 | 0.06 | 0.06 | 0.09 | 0.09 | 0.10 | 0.09 | 0.09 | 0.08 | 0.14 |
| Muon scale | 0.03 | 0.03 | 0.03 | 0.03 | 0.03 | 0.03 | 0.03 | 0.04 | 0.04 | 0.03 | 0.03 |
| QCD $+/-$ | 0.15 | 0.15 | 0.15 | 0.15 | 0.15 | 0.15 | 0.16 | 0.18 | 0.17 | 0.14 | 0.10 |
| QCD shape | 0.02 | 0.03 | 0.03 | 0.03 | 0.04 | 0.04 | 0.05 | 0.06 | 0.07 | 0.05 | 0.04 |
| EW+$t\bar{t}$ bkg | 0.03 | 0.03 | 0.03 | 0.03 | 0.03 | 0.03 | 0.03 | 0.03 | 0.04 | 0.04 | 0.05 |
| $\not{E}_T$ shape | 0.03 | 0.04 | 0.04 | 0.04 | 0.05 | 0.06 | 0.06 | 0.09 | 0.09 | 0.09 | 0.07 |
| PDF | 0.03 | 0.02 | 0.02 | 0.02 | 0.02 | 0.03 | 0.04 | 0.05 | 0.05 | 0.09 | 0.08 |
| FSR | 0.00 | 0.00 | 0.00 | 0.00 | 0.00 | 0.00 | 0.00 | 0.00 | 0.00 | 0.00 | 0.01 |
| Total syst. | 0.17 | 0.18 | 0.18 | 0.18 | 0.19 | 0.20 | 0.22 | 0.23 | 0.23 | 0.22 | 0.21 |
| Stat. | 0.06 | 0.06 | 0.06 | 0.06 | 0.06 | 0.07 | 0.07 | 0.07 | 0.06 | 0.06 | 0.07 |
| Total unc. | 0.18 | 0.19 | 0.19 | 0.19 | 0.20 | 0.21 | 0.23 | 0.24 | 0.24 | 0.23 | 0.22 |

CT10 error set is used to estimate the correlations between the two charges and different $|\eta|$ bins.

Finally, a $\pm 2.6\%$ uncertainty [37] is assigned to the integrated luminosity of the data sample. The luminosity uncertainty is fully correlated between the $|\eta|$ bins and two charges. Therefore, this uncertainty cancels in the measured charge asymmetries. The uncertainty in the normalization of the electroweak backgrounds due to the luminosity uncertainty has a negligible impact on the measurements.

Table 2 summarizes the systematic uncertainties in the measured cross sections and asymmetries. For comparison, the statistical and luminosity uncertainties are also shown. The uncertainty in the integrated luminosity dominates the total uncertainties in the measured cross sections, while the uncertainty in the QCD background estimation dominates the uncertainties in the charge asymmetries. The uncertainties for the muon charge asymmetries are calculated

Table 3: Correlation matrices of systematic uncertainties for $\sigma_\eta^\pm$ and $\mathcal{A}$. The statistical and integrated luminosity uncertainties are not included. The full $22 \times 22$ correlation matrix for $\sigma_\eta^\pm$ is presented as four blocks of $11 \times 11$ matrices, as shown in Eq. (4). The $C_{++}$ and $C_{--}$ blocks on the diagonal represent the bin-to-bin correlations of $\delta\sigma_\eta^+$ and $\delta\sigma_\eta^-$, respectively. The off-diagonal $C_{+-}$ and $C_{+-}^T$ blocks describe the correlations between the two charges. The values are expressed as percentages.

| $\lvert\eta\rvert$ bin | 0.0–0.2 | 0.2–0.4 | 0.4–0.6 | 0.6–0.8 | 0.8–1.0 | 1.0–1.2 | 1.2–1.4 | 1.4–1.6 | 1.6–1.85 | 1.85–2.1 | 2.1–2.4 |
|---|---|---|---|---|---|---|---|---|---|---|---|
| Correlation matrix of systematic uncertainties in $\sigma_\eta^\pm$ | | | | | | | | | | | |
| $C_{++}$ | | | | | | | | | | | |
| 0.00–0.20 | 100.0 | 90.3 | 91.3 | 91.2 | 90.2 | 81.8 | 69.4 | 63.3 | 32.9 | 6.1 | −37.2 |
| 0.20–0.40 | | 100.0 | 92.5 | 92.4 | 92.2 | 74.9 | 58.6 | 51.1 | 16.2 | −11.8 | −54.7 |
| 0.40–0.60 | | | 100.0 | 92.5 | 92.1 | 79.2 | 64.8 | 57.9 | 25.0 | −2.8 | −46.6 |
| 0.60–0.80 | | | | 100.0 | 92.2 | 79.5 | 65.4 | 58.6 | 25.8 | −1.9 | −46.0 |
| 0.80–1.00 | | | | | 100.0 | 78.3 | 63.7 | 56.7 | 23.2 | −4.5 | −48.7 |
| 1.00–1.20 | | | | | | 100.0 | 82.8 | 79.9 | 60.0 | 38.5 | −3.9 |
| 1.20–1.40 | | | | | | | 100.0 | 85.6 | 74.8 | 58.4 | 20.5 |
| 1.40–1.60 | | | | | | | | 100.0 | 79.8 | 65.6 | 30.0 |
| 1.60–1.85 | | | | | | | | | 100.0 | 86.6 | 64.5 |
| 1.85–2.10 | | | | | | | | | | 100.0 | 83.8 |
| 2.10–2.40 | | | | | | | | | | | 100.0 |
| $C_{--}$ | | | | | | | | | | | |
| 0.00–0.20 | 100.0 | 91.1 | 92.1 | 91.9 | 91.2 | 81.8 | 64.8 | 65.6 | 38.5 | 19.0 | −31.5 |
| 0.20–0.40 | | 100.0 | 92.8 | 92.3 | 91.2 | 74.6 | 53.0 | 54.4 | 23.1 | 2.2 | −48.8 |
| 0.40–0.60 | | | 100.0 | 92.8 | 92.1 | 80.1 | 61.2 | 62.5 | 33.3 | 12.8 | −38.7 |
| 0.60–0.80 | | | | 100.0 | 92.3 | 81.3 | 63.4 | 64.6 | 36.2 | 15.8 | −35.9 |
| 0.80–1.00 | | | | | 100.0 | 82.5 | 65.4 | 66.8 | 39.0 | 18.6 | −33.3 |
| 1.00–1.20 | | | | | | 100.0 | 83.5 | 84.1 | 67.9 | 52.2 | 5.4 |
| 1.20–1.40 | | | | | | | 100.0 | 88.9 | 83.9 | 73.2 | 35.4 |
| 1.40–1.60 | | | | | | | | 100.0 | 83.8 | 72.6 | 33.1 |
| 1.60–1.85 | | | | | | | | | 100.0 | 88.5 | 64.4 |
| 1.85–2.10 | | | | | | | | | | 100.0 | 80.4 |
| 2.10–2.40 | | | | | | | | | | | 100.0 |
| $C_{+-}$ | | | | | | | | | | | |
| 0.00–0.20 | 92.7 | 89.5 | 90.1 | 89.9 | 89.0 | 78.7 | 61.1 | 61.7 | 34.6 | 16.0 | −32.9 |
| 0.20–0.40 | 88.9 | 94.4 | 90.7 | 90.1 | 88.8 | 71.2 | 49.0 | 50.1 | 18.8 | −1.2 | −50.5 |
| 0.40–0.60 | 90.0 | 91.7 | 93.6 | 90.9 | 89.9 | 76.0 | 55.9 | 56.9 | 27.4 | 7.6 | −42.2 |
| 0.60–0.80 | 89.7 | 91.4 | 90.9 | 93.2 | 89.9 | 76.2 | 56.4 | 57.3 | 28.1 | 8.3 | −41.6 |
| 0.80–1.00 | 88.8 | 91.3 | 90.5 | 90.4 | 92.0 | 74.9 | 54.6 | 55.7 | 25.9 | 5.9 | −44.1 |
| 1.00–1.20 | 80.4 | 74.4 | 78.8 | 80.1 | 80.8 | 87.9 | 77.4 | 77.4 | 60.4 | 45.7 | 0.8 |
| 1.20–1.40 | 68.5 | 58.5 | 65.4 | 67.3 | 68.7 | 82.1 | 86.3 | 82.8 | 74.5 | 63.8 | 25.2 |
| 1.40–1.60 | 62.6 | 51.2 | 59.0 | 61.2 | 62.9 | 80.1 | 84.7 | 86.4 | 79.6 | 70.5 | 34.8 |
| 1.60–1.85 | 32.7 | 16.8 | 26.9 | 29.8 | 32.2 | 61.8 | 78.4 | 77.1 | 89.1 | 87.0 | 68.2 |
| 1.85–2.10 | 6.0 | −11.4 | −0.8 | 2.3 | 4.9 | 40.4 | 63.9 | 61.7 | 82.1 | 91.4 | 86.0 |
| 2.10–2.40 | −36.9 | −54.0 | −44.2 | −41.7 | −39.3 | −1.0 | 29.0 | 26.2 | 58.5 | 75.1 | 98.2 |
| Correlation matrix of systematic uncertainties in $\mathcal{A}$ | | | | | | | | | | | |
| 0.00–0.20 | 100.0 | 27.2 | 27.4 | 26.8 | 24.8 | 26.7 | 24.3 | 27.0 | 26.1 | 25.0 | 19.7 |
| 0.20–0.40 | | 100.0 | 27.8 | 27.2 | 24.5 | 27.3 | 24.1 | 28.9 | 27.8 | 28.1 | 22.5 |
| 0.40–0.60 | | | 100.0 | 28.3 | 27.4 | 28.6 | 27.0 | 29.9 | 29.5 | 28.0 | 21.4 |
| 0.60–0.80 | | | | 100.0 | 29.3 | 29.0 | 29.1 | 30.6 | 30.9 | 28.7 | 22.2 |
| 0.80–1.00 | | | | | 100.0 | 29.7 | 32.8 | 32.0 | 33.0 | 28.4 | 20.7 |
| 1.00–1.20 | | | | | | 100.0 | 31.2 | 33.6 | 34.3 | 31.9 | 25.4 |
| 1.20–1.40 | | | | | | | 100.0 | 34.2 | 36.8 | 30.6 | 25.1 |
| 1.40–1.60 | | | | | | | | 100.0 | 39.1 | 37.4 | 31.0 |
| 1.60–1.85 | | | | | | | | | 100.0 | 38.6 | 33.3 |
| 1.85–2.10 | | | | | | | | | | 100.0 | 42.0 |
| 2.10–2.40 | | | | | | | | | | | 100.0 |

from those in the differential cross sections, taking into account the correlations between the two charges.

The correlations in the systematic uncertainty between the charges and different $|\eta|$ bins are shown in Table 3. The full $22 \times 22$ correlation matrix $C$ is split into four $11 \times 11$ blocks as

$$C = \begin{bmatrix} C_{++} & C_{+-} \\ C_{+-}^T & C_{--} \end{bmatrix}, \tag{4}$$

where the $C_{++}$ and $C_{--}$ matrices represent the bin-to-bin correlations of systematic uncertainties in $\sigma_\eta^+$ and $\sigma_\eta^-$, respectively, and $C_{+-}$ describes the correlations between the two charges. To construct the total covariance matrix, the covariance matrix of the systematic uncertainties should be added to those of the statistical and integrated luminosity uncertainties. The latter are fully correlated between the two charges and $|\eta|$ bins. For the statistical uncertainties bin-to-bin correlations are zero; the correlations between the two charges are shown in Table 1.

# 7 Results

The measured cross sections and charge asymmetries are summarized in Table 4 and displayed in Fig. 2. The error bars of the measurements represent both statistical and systematic uncertainties, including the uncertainty in the integrated luminosity. The measurements are compared with theoretical predictions based on several PDF sets. The predictions are obtained using the FEWZ 3.1 [38] NNLO MC calculation interfaced with CT10 [18], NNPDF3.0 [39], HERAPDF1.5 [40], MMHT2014 [41], and ABM12 [42] PDF sets. No electroweak corrections are included in these calculations. The error bars of the theoretical predictions represent the PDF uncertainty, which is the dominant source of uncertainty in these calculations. For the CT10, MMHT, HERA, and ABM PDFs, the uncertainties are calculated with their eigenvector sets using asymmetric master equations where applicable. For the NNPDF set the standard deviations over its 100 replicas are evaluated.

The numerical values of the predictions are also shown in Table 4. We note that the previous lepton charge asymmetries measured by CMS at $\sqrt{s} = 7$ TeV have been included in the global PDF fits for the NNPDF3.0, MMHT2014, and ABM12 PDFs. The measured cross sections and charge asymmetries are well described by all considered PDF sets within their corresponding uncertainties.

# 8 QCD analysis

The muon charge asymmetry measurements at 8 TeV presented here are used in a QCD analysis at NNLO together with the combined measurements of neutral- and charged-current cross sections of deep inelastic electron(positron)-proton scattering (DIS) at HERA [43]. The correlations of the experimental uncertainties for the muon charge asymmetry and for the inclusive DIS cross sections are taken into account. The theoretical predictions are calculated at NLO by using the MCFM 6.8 program [44, 45], which is interfaced to APPLGRID 1.4.56 [46]. The NNLO corrections are obtained by using $k$-factors, defined as ratios of the predictions at NNLO to the ones at NLO, both calculated with the FEWZ 3.1 [38] program, using NNLO CT10 [18] PDFs.

Version 1.1.1 of the open-source QCD fit framework for PDF determination HERAFitter [47, 48] is used with the partons evolved by using the Dokshitzer-Gribov-Lipatov-Altarelli-Parisi equations [49–54] at NNLO, as implemented in the QCDNUM 17-00/06 program [55].

Table 4: Summary of the measured differential cross sections $\sigma_\eta^\pm$ (pb) and charge asymmetry $\mathcal{A}$. The first uncertainty is statistical, the second uncertainty is systematic, and the third is the integrated luminosity uncertainty. The theoretical predictions are obtained using the FEWZ 3.1 [38] NNLO MC tool interfaced with five different PDF sets.

| | Measurement | Theory | | | | |
|---|---|---|---|---|---|---|
| $\lvert\eta\rvert$ bin | ($\pm$ stat $\pm$ syst $\pm$ lumi) | CT10 | NNPDF3.0 | MMHT2014 | ABM12 | HERAPDF1.5 |
| | | | $\sigma_\eta^+$ (pb) | | | |
| 0.00–0.20 | $743.7 \pm 0.7 \pm 6.5 \pm 19.3$ | $759.7^{+19.3}_{-25.1}$ | $740.5 \pm 16.8$ | $750.8^{+13.2}_{-10.8}$ | $764.2 \pm 9.3$ | $762.8^{+6.8}_{-7.8}$ |
| 0.20–0.40 | $749.5 \pm 0.7 \pm 7.7 \pm 19.5$ | $761.2^{+19.2}_{-24.9}$ | $740.8 \pm 16.6$ | $751.8^{+13.1}_{-10.6}$ | $766.0 \pm 9.6$ | $764.7^{+7.2}_{-7.8}$ |
| 0.40–0.60 | $751.9 \pm 0.7 \pm 7.2 \pm 19.5$ | $763.6^{+19.1}_{-24.6}$ | $743.5 \pm 16.5$ | $754.0^{+13.0}_{-10.3}$ | $769.4 \pm 9.7$ | $767.9^{+6.5}_{-6.6}$ |
| 0.60–0.80 | $755.0 \pm 0.7 \pm 7.1 \pm 19.6$ | $769.1^{+18.6}_{-23.8}$ | $746.9 \pm 16.0$ | $759.0^{+13.1}_{-10.1}$ | $773.8 \pm 9.4$ | $772.0^{+7.8}_{-7.2}$ |
| 0.80–1.00 | $761.9 \pm 0.7 \pm 7.4 \pm 19.8$ | $773.4^{+18.2}_{-22.8}$ | $750.7 \pm 16.0$ | $763.6^{+13.0}_{-9.8}$ | $780.0 \pm 9.9$ | $777.5^{+7.6}_{-6.4}$ |
| 1.00–1.20 | $766.0 \pm 0.7 \pm 5.8 \pm 19.9$ | $777.8^{+17.7}_{-22.1}$ | $756.5 \pm 15.8$ | $769.2^{+12.8}_{-9.8}$ | $784.9 \pm 9.7$ | $782.5^{+8.2}_{-6.8}$ |
| 1.20–1.40 | $774.4 \pm 0.7 \pm 5.8 \pm 20.1$ | $785.0^{+17.7}_{-21.5}$ | $760.9 \pm 15.6$ | $775.5^{+13.1}_{-10.5}$ | $791.5 \pm 9.9$ | $787.3^{+8.7}_{-6.8}$ |
| 1.40–1.60 | $774.6 \pm 0.7 \pm 6.1 \pm 20.1$ | $793.7^{+17.5}_{-20.8}$ | $768.5 \pm 15.7$ | $784.0^{+13.3}_{-11.3}$ | $799.7 \pm 10.2$ | $796.7^{+11.4}_{-9.5}$ |
| 1.60–1.85 | $776.4 \pm 0.7 \pm 6.8 \pm 20.2$ | $784.4^{+16.9}_{-19.5}$ | $761.3 \pm 15.4$ | $778.5^{+13.5}_{-12.4}$ | $792.4 \pm 10.3$ | $788.9^{+15.0}_{-11.5}$ |
| 1.85–2.10 | $771.1 \pm 0.6 \pm 7.9 \pm 20.0$ | $785.5^{+16.9}_{-18.8}$ | $762.2 \pm 15.7$ | $780.3^{+14.0}_{-14.0}$ | $791.6 \pm 10.2$ | $788.9^{+17.6}_{-11.4}$ |
| 2.10–2.40 | $748.3 \pm 0.7 \pm 18.0 \pm 19.5$ | $750.0^{+16.4}_{-17.7}$ | $730.1 \pm 15.4$ | $746.9^{+13.9}_{-14.6}$ | $755.6 \pm 9.6$ | $754.8^{+20.9}_{-12.3}$ |
| | | | $\sigma_\eta^-$ (pb) | | | |
| 0.00–0.20 | $569.0 \pm 0.6 \pm 5.3 \pm 14.8$ | $574.5^{+14.5}_{-20.2}$ | $562.2 \pm 13.3$ | $576.2^{+9.4}_{-10.1}$ | $580.2 \pm 7.2$ | $578.8^{+4.1}_{-7.6}$ |
| 0.20–0.40 | $568.9 \pm 0.6 \pm 6.4 \pm 14.8$ | $571.0^{+14.6}_{-20.1}$ | $559.6 \pm 13.3$ | $573.2^{+9.6}_{-10.3}$ | $577.4 \pm 7.4$ | $576.1^{+5.0}_{-8.1}$ |
| 0.40–0.60 | $564.1 \pm 0.6 \pm 5.7 \pm 14.7$ | $566.4^{+14.2}_{-19.3}$ | $555.6 \pm 12.8$ | $569.7^{+8.8}_{-9.3}$ | $572.6 \pm 6.9$ | $572.5^{+4.1}_{-7.2}$ |
| 0.60–0.80 | $556.1 \pm 0.6 \pm 5.5 \pm 14.5$ | $558.6^{+13.7}_{-18.3}$ | $547.5 \pm 12.4$ | $561.8^{+8.6}_{-8.9}$ | $565.9 \pm 7.2$ | $565.7^{+5.8}_{-8.0}$ |
| 0.80–1.00 | $549.6 \pm 0.6 \pm 5.5 \pm 14.3$ | $548.6^{+13.4}_{-17.3}$ | $538.8 \pm 11.7$ | $553.6^{+8.3}_{-8.3}$ | $557.9 \pm 7.0$ | $557.4^{+4.9}_{-7.0}$ |
| 1.00–1.20 | $535.7 \pm 0.6 \pm 4.6 \pm 13.9$ | $535.6^{+12.8}_{-16.0}$ | $526.6 \pm 11.6$ | $542.2^{+8.0}_{-8.1}$ | $544.2 \pm 6.8$ | $547.2^{+5.3}_{-7.0}$ |
| 1.20–1.40 | $521.4 \pm 0.6 \pm 4.6 \pm 13.6$ | $521.8^{+12.4}_{-14.9}$ | $512.4 \pm 10.9$ | $527.5^{+8.0}_{-8.2}$ | $530.9 \pm 6.6$ | $534.5^{+5.3}_{-7.0}$ |
| 1.40–1.60 | $508.3 \pm 0.6 \pm 4.9 \pm 13.2$ | $509.3^{+11.8}_{-13.9}$ | $500.6 \pm 10.5$ | $516.3^{+8.2}_{-8.4}$ | $519.3 \pm 6.5$ | $524.2^{+5.4}_{-6.7}$ |
| 1.60–1.85 | $487.7 \pm 0.6 \pm 5.2 \pm 12.7$ | $485.1^{+11.2}_{-12.6}$ | $478.1 \pm 9.9$ | $492.5^{+8.6}_{-8.8}$ | $494.6 \pm 6.0$ | $501.6^{+6.3}_{-6.6}$ |
| 1.85–2.10 | $466.6 \pm 0.6 \pm 5.3 \pm 12.1$ | $467.0^{+11.0}_{-11.7}$ | $459.9 \pm 9.4$ | $473.8^{+9.1}_{-9.4}$ | $475.1 \pm 5.6$ | $483.4^{+8.7}_{-7.3}$ |
| 2.10–2.40 | $439.8 \pm 0.6 \pm 10.6 \pm 11.4$ | $436.0^{+10.6}_{-11.1}$ | $431.0 \pm 9.0$ | $442.3^{+9.1}_{-9.4}$ | $442.0 \pm 5.3$ | $452.4^{+10.1}_{-6.6}$ |
| | | | $\mathcal{A}$ (%) | | | |
| 0.00–0.20 | $13.31 \pm 0.06 \pm 0.17$ | $13.89^{+0.55}_{-0.57}$ | $13.68 \pm 0.25$ | $13.16^{+0.48}_{-0.30}$ | $13.69 \pm 0.20$ | $13.71^{+0.50}_{-0.43}$ |
| 0.20–0.40 | $13.70 \pm 0.06 \pm 0.18$ | $14.28^{+0.56}_{-0.59}$ | $13.94 \pm 0.23$ | $13.48^{+0.49}_{-0.30}$ | $14.04 \pm 0.20$ | $14.07^{+0.51}_{-0.44}$ |
| 0.40–0.60 | $14.27 \pm 0.06 \pm 0.18$ | $14.83^{+0.56}_{-0.60}$ | $14.47 \pm 0.21$ | $13.92^{+0.48}_{-0.30}$ | $14.66 \pm 0.23$ | $14.58^{+0.53}_{-0.45}$ |
| 0.60–0.80 | $15.18 \pm 0.06 \pm 0.18$ | $15.85^{+0.55}_{-0.61}$ | $15.40 \pm 0.19$ | $14.93^{+0.49}_{-0.30}$ | $15.52 \pm 0.21$ | $15.42^{+0.54}_{-0.47}$ |
| 0.80–1.00 | $16.19 \pm 0.06 \pm 0.19$ | $17.01^{+0.57}_{-0.64}$ | $16.44 \pm 0.19$ | $15.95^{+0.50}_{-0.31}$ | $16.59 \pm 0.22$ | $16.49^{+0.58}_{-0.50}$ |
| 1.00–1.20 | $17.69 \pm 0.07 \pm 0.20$ | $18.44^{+0.55}_{-0.65}$ | $17.92 \pm 0.19$ | $17.31^{+0.51}_{-0.34}$ | $18.11 \pm 0.21$ | $17.69^{+0.58}_{-0.51}$ |
| 1.20–1.40 | $19.52 \pm 0.07 \pm 0.22$ | $20.14^{+0.56}_{-0.67}$ | $19.52 \pm 0.20$ | $19.03^{+0.53}_{-0.38}$ | $19.70 \pm 0.23$ | $19.13^{+0.62}_{-0.54}$ |
| 1.40–1.60 | $20.75 \pm 0.07 \pm 0.23$ | $21.82^{+0.56}_{-0.68}$ | $21.10 \pm 0.21$ | $20.59^{+0.55}_{-0.42}$ | $21.26 \pm 0.23$ | $20.63^{+0.60}_{-0.54}$ |
| 1.60–1.85 | $22.83 \pm 0.06 \pm 0.23$ | $23.57^{+0.55}_{-0.68}$ | $22.84 \pm 0.23$ | $22.50^{+0.57}_{-0.48}$ | $23.14 \pm 0.23$ | $22.26^{+0.63}_{-0.55}$ |
| 1.85–2.10 | $24.61 \pm 0.06 \pm 0.22$ | $25.43^{+0.54}_{-0.67}$ | $24.74 \pm 0.25$ | $24.44^{+0.57}_{-0.52}$ | $24.99 \pm 0.24$ | $24.01^{+0.69}_{-0.60}$ |
| 2.10–2.40 | $25.96 \pm 0.07 \pm 0.21$ | $26.47^{+0.50}_{-0.62}$ | $25.75 \pm 0.28$ | $25.61^{+0.57}_{-0.55}$ | $26.19 \pm 0.29$ | $25.05^{+0.78}_{-0.67}$ |

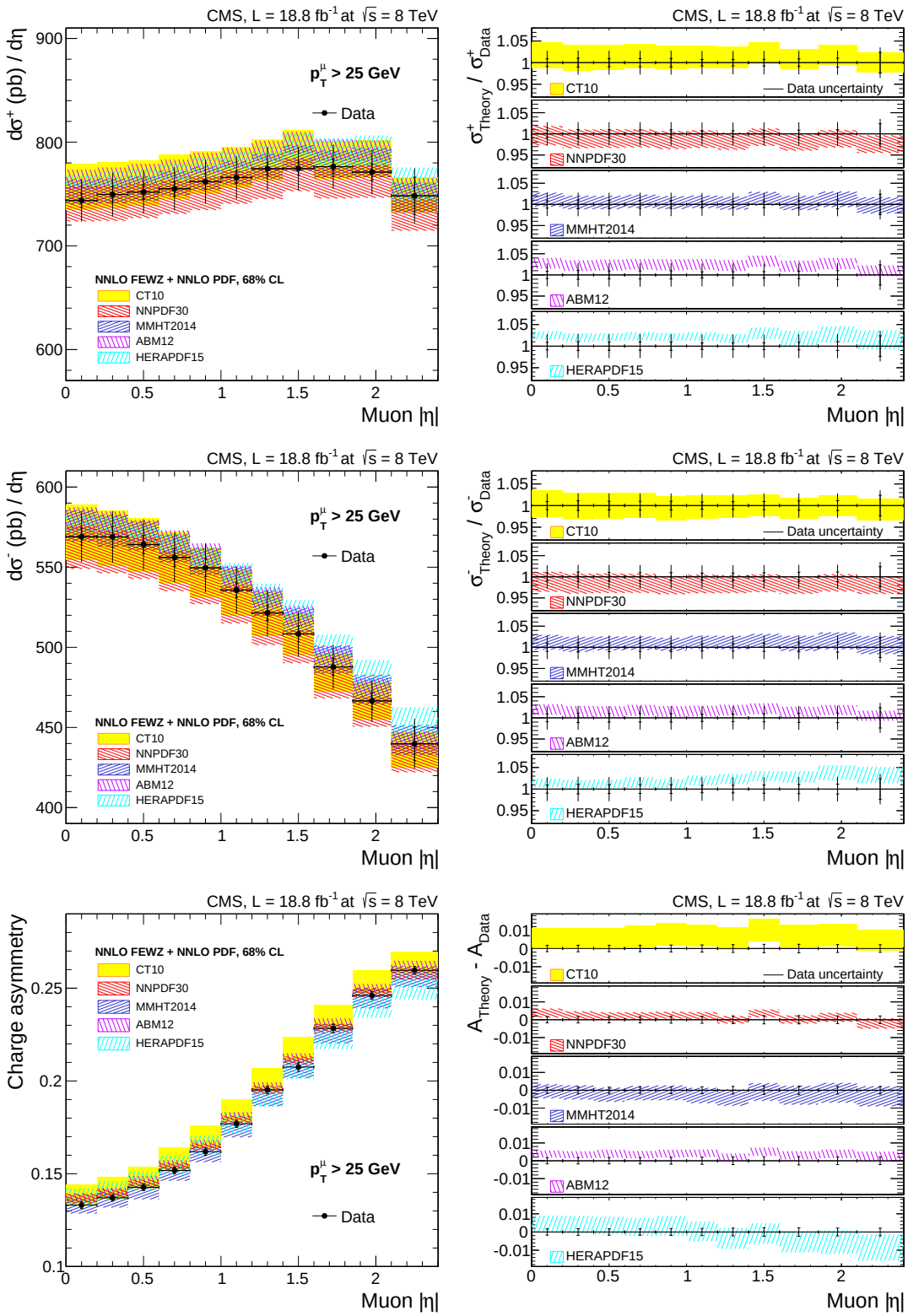


Figure 2: Comparison of the measured cross sections (upper plot for $\sigma_\eta^+$ and middle for $\sigma_\eta^-$) and asymmetries (lower plot) to NNLO predictions calculated using the FEWZ 3.1 MC tool interfaced with different PDF sets. The right column shows the ratios (differences) between the theoretical predictions and the measured cross sections (asymmetries). The smaller vertical error bars on the data points represent the statistical and systematic uncertainties. The full error bars include the integrated luminosity uncertainty. The PDF uncertainty of each PDF set is shown by a shaded (or hatched) band and corresponds to 68% CL.

The Thorne-Roberts [35, 56] general mass variable flavor number scheme at NNLO is used for the treatment of heavy-quark contributions with heavy-quark masses $m_c = 1.43\,\mathrm{GeV}$ and $m_b = 4.5\,\mathrm{GeV}$. The renormalization and factorization scales are set to $Q$, which denotes the four-momentum transfer in case of the DIS data and the mass of the W boson in case of the muon charge asymmetry, respectively.

The strong coupling constant is set to $\alpha_s(m_Z) = 0.118$. The $Q^2$ range of HERA data is restricted to $Q^2 \geq Q^2_{\mathrm{min}} = 3.5\,\mathrm{GeV}^2$ to assure the applicability of perturbative QCD over the kinematic range of the fit.

The procedure for the determination of the PDFs follows the approach used in the analysis in Ref. [11]. The parameterised PDFs are the gluon distribution, $x\mathrm{g}$, the valence quark distributions, $x\mathrm{u}_v$, $x\mathrm{d}_v$, and the u-type and d-type anti-quark distributions, $x\overline{U}$, $x\overline{D}$. At the initial scale of the QCD evolution $Q_0^2 = 1.9\,\mathrm{GeV}^2$, the PDFs are parametrized as:

$$
\begin{aligned}
x\mathrm{g}(x) &= A_{\mathrm{g}} x^{B_{\mathrm{g}}} (1-x)^{C_{\mathrm{g}}} (1 + D_{\mathrm{g}} x), && (5)\\
x\mathrm{u}_v(x) &= A_{\mathrm{u}_v} x^{B_{\mathrm{u}_v}} (1-x)^{C_{\mathrm{u}_v}} (1 + E_{\mathrm{u}_v} x^2), && (6)\\
x\mathrm{d}_v(x) &= A_{\mathrm{d}_v} x^{B_{\mathrm{d}_v}} (1-x)^{C_{\mathrm{d}_v}}, && (7)\\
x\overline{U}(x) &= A_{\overline{U}} x^{B_{\overline{U}}} (1-x)^{C_{\overline{U}}} (1 + E_{\overline{U}} x^2), && (8)\\
x\overline{D}(x) &= A_{\overline{D}} x^{B_{\overline{D}}} (1-x)^{C_{\overline{D}}}, && (9)
\end{aligned}
$$

with the relations $x\overline{U} = x\overline{\mathrm{u}}$ and $x\overline{D} = x\overline{\mathrm{d}} + x\overline{\mathrm{s}}$ assumed.

The normalization parameters $A_{\mathrm{u_v}}$, $A_{\mathrm{d_v}}$, and $A_{\mathrm{g}}$ are determined by the QCD sum rules, the $B$ parameter is responsible for small-$x$ behavior of the PDFs, and the parameter $C$ describes the shape of the distribution as $x \to 1$. Additional constraints $B_{\overline{\mathrm{U}}} = B_{\overline{\mathrm{D}}}$ and $A_{\overline{\mathrm{U}}} = A_{\overline{\mathrm{D}}}(1 - f_{\mathrm{s}})$ are imposed with $f_{\mathrm{s}}$ being the strangeness fraction, $f_{\mathrm{s}} = \overline{\mathrm{s}}/(\overline{\mathrm{d}} + \overline{\mathrm{s}})$, which is fixed to $f_{\mathrm{s}} = 0.31 \pm 0.08$ as in Ref. [35], consistent with the determination of the strangeness fraction by using the CMS measurements of W + charm production [11]. The $\chi^2$ definition in the QCD analysis follows that of Eq.(32) of [43] without the logarithmic term. The parameters in Eqs. (5)-(9) were selected by first fitting with all $D$ and $E$ parameters set to zero. The other parameters were then included in the fit one at a time independently. The improvement of the $\chi^2$ of the fits was monitored and the procedure was stopped when no further improvement was observed. This led to a 13-parameter fit.

The PDF uncertainties are estimated according to the general approach of HERAPDF1.0 [57] in which the experimental, model, and parametrization uncertainties are taken into account. A tolerance criterion of $\Delta\chi^2 = 1$ is adopted for defining the experimental uncertainties that originate from the measurements included in the analysis.

Model uncertainties arise from the variations in the values assumed for the heavy-quark masses $m_b$, $m_c$ with $4.25 \leq m_b \leq 4.75\,\mathrm{GeV}$, $1.37 \leq m_c \leq 1.49\,\mathrm{GeV}$, following Ref. [43], and the value of $Q^2_{\mathrm{min}}$ imposed on the HERA data, which is varied in the interval $2.5 \leq Q^2_{\mathrm{min}} \leq 5.0\,\mathrm{GeV}^2$. The strangeness fraction $f_{\mathrm{s}}$ is varied by its uncertainty.

The parametrization uncertainty is estimated by extending the functional form of all parton densities with additional parameters. The uncertainty is constructed as an envelope built from the maximal differences between the PDFs resulting from all the parametrization variations and the central fit at each $x$ value. The total PDF uncertainty is obtained by adding experimental, model, and parametrization uncertainties in quadrature. In the following, the quoted uncertainties correspond to 68% CL.

Table 5: Partial $\chi^2$ per number of data points, $n_{\mathrm{dp}}$, and the global $\chi^2$ per degrees of freedom, $n_{\mathrm{dof}}$, as obtained in the QCD analysis of HERA DIS and the CMS muon charge asymmetry data. For HERA measurements, the energy of the proton beam is listed for each data set, with electron energy being $E_{\mathrm{e}} = 27.5\,\mathrm{GeV}$.

| Data sets | Partial $\chi^2/n_{\mathrm{dp}}$ |
|---|---|
| HERA1+2 neutral current, $\mathrm{e}^+\mathrm{p}$, $E_{\mathrm{p}} = 920\,\mathrm{GeV}$ | 440/377 |
| HERA1+2 neutral current, $\mathrm{e}^+\mathrm{p}$, $E_{\mathrm{p}} = 820\,\mathrm{GeV}$ | 69/70 |
| HERA1+2 neutral current, $\mathrm{e}^+\mathrm{p}$, $E_{\mathrm{p}} = 575\,\mathrm{GeV}$ | 214/254 |
| HERA1+2 neutral current, $\mathrm{e}^+\mathrm{p}$, $E_{\mathrm{p}} = 460\,\mathrm{GeV}$ | 210/204 |
| HERA1+2 neutral current, $\mathrm{e}^-\mathrm{p}$, $E_{\mathrm{p}} = 920\,\mathrm{GeV}$ | 218/159 |
| HERA1+2 charged current, $\mathrm{e}^+\mathrm{p}$, $E_{\mathrm{p}} = 920\,\mathrm{GeV}$ | 46/39 |
| HERA1+2 charged current, $\mathrm{e}^-\mathrm{p}$, $E_{\mathrm{p}} = 920\,\mathrm{GeV}$ | 50/42 |
| CMS $\mathrm{W}^\pm$ muon charge asymmetry $\mathcal{A}(\eta\mu)$, $\sqrt{s} = 8\,\mathrm{TeV}$ | 3/11 |
| Correlated $\chi^2$ | 141 |
| Global $\chi^2/n_{\mathrm{dof}}$ | 1391/1143 |

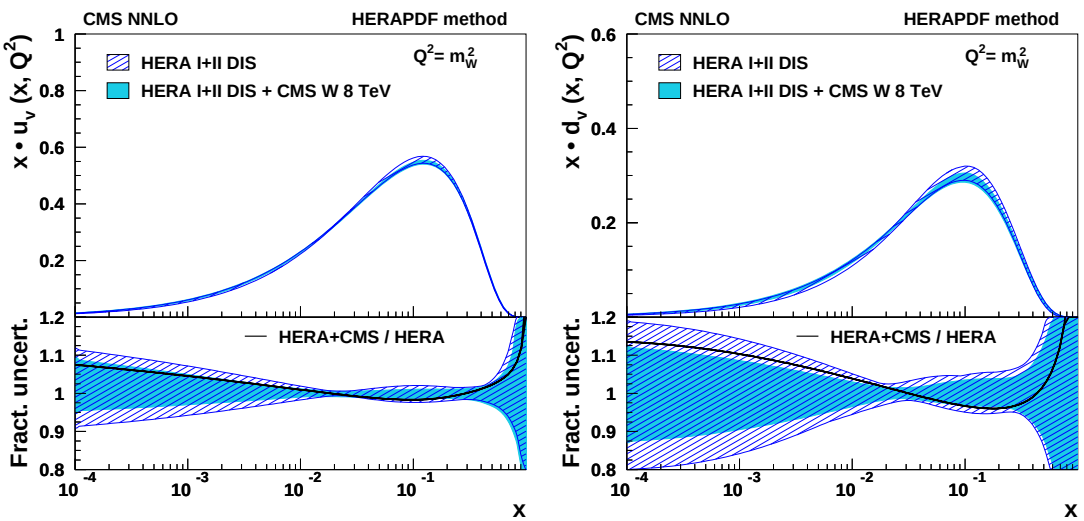


Figure 3: Distributions of u valence (left) and d valence (right) quarks as functions of $x$ at the scale $Q^2 = m_{\mathrm{W}}^2$. The results of the fit to the HERA data and muon asymmetry measurements (light shaded band), and to HERA data only (hatched band) are compared. The total PDF uncertainties are shown. In the bottom panels the distributions are normalized to 1 for a direct comparison of the uncertainties. The change of the PDFs with respect to the HERA-only fit is represented by a solid line.

The global and partial $\chi^2$ values for the data sets used are listed in Table 5, illustrating the consistency among the data sets used. The somewhat high $\chi^2/n_{\mathrm{dof}}$ values for the combined DIS data are very similar to those observed in Ref. [43], where they are investigated in detail.

In the kinematic range probed, the final combined HERA DIS data currently provide the most significant constraints on the valence distributions. By adding these muon charge asymmetry measurements, the constraints can be significantly improved, as illustrated in Fig. 3 where the $x$u and $x$d valence distributions are shown at the scale of $m_{\mathrm{W}}^2$, relevant for the W boson production. The changes in shapes and the reduction of the uncertainties of the valence quark distributions with respect to those obtained with the HERA data are clear.

## 9 Summary

In summary, we have measured the differential cross section and charge asymmetry of the $\mathrm{W}^{\pm} \to \mu^{\pm}\nu$ production in pp collisions at $\sqrt{s} = 8\,\mathrm{TeV}$ using a data sample corresponding to an integrated luminosity of $18.8\,\mathrm{fb}^{-1}$ collected with the CMS detector at the LHC. The measurements were performed in 11 bins of absolute muon pseudorapidity $|\eta|$ for muons with $p_{\mathrm{T}} > 25\,\mathrm{GeV}$. The results have been incorporated into a QCD analysis at next-to-next-to-leading-order together with the inclusive deep inelastic scattering data from HERA. A significant improvement in the accuracy of the valence quark distributions is observed in the range $10^{-3} < x < 10^{-1}$, demonstrating the power of these muon charge asymmetry measurements to improve the main constraints on the valence distributions imposed by the HERA data, in the kinematics range probed. This strongly suggests the use of these measurements in future PDF determinations.

## Acknowledgments

We congratulate our colleagues in the CERN accelerator departments for the excellent performance of the LHC and thank the technical and administrative staffs at CERN and at other CMS institutes for their contributions to the success of the CMS effort. In addition, we gratefully acknowledge the computing centres and personnel of the Worldwide LHC Computing Grid for delivering so effectively the computing infrastructure essential to our analyses. Finally, we acknowledge the enduring support for the construction and operation of the LHC and the CMS detector provided by the following funding agencies: BMWFW and FWF (Austria); FNRS and FWO (Belgium); CNPq, CAPES, FAPERJ, and FAPESP (Brazil); MES (Bulgaria); CERN; CAS, MoST, and NSFC (China); COLCIENCIAS (Colombia); MSES and CSF (Croatia); RPF (Cyprus); MoER, ERC IUT and ERDF (Estonia); Academy of Finland, MEC, and HIP (Finland); CEA and CNRS/IN2P3 (France); BMBF, DFG, and HGF (Germany); GSRT (Greece); OTKA and NIH (Hungary); DAE and DST (India); IPM (Iran); SFI (Ireland); INFN (Italy); MSIP and NRF (Republic of Korea); LAS (Lithuania); MOE and UM (Malaysia); CINVESTAV, CONACYT, SEP, and UASLP-FAI (Mexico); MBIE (New Zealand); PAEC (Pakistan); MSHE and NSC (Poland); FCT (Portugal); JINR (Dubna); MON, RosAtom, RAS and RFBR (Russia); MESTD (Serbia); SEIDI and CPAN (Spain); Swiss Funding Agencies (Switzerland); MST (Taipei); ThEPCenter, IPST, STAR and NSTDA (Thailand); TUBITAK and TAEK (Turkey); NASU and SFFR (Ukraine); STFC (United Kingdom); DOE and NSF (USA).

Individuals have received support from the Marie-Curie programme and the European Research Council and EPLANET (European Union); the Leventis Foundation; the A. P. Sloan Foundation; the Alexander von Humboldt Foundation; the Belgian Federal Science Policy Office; the Fonds pour la Formation à la Recherche dans l'Industrie et dans l'Agriculture (FRIA-

Belgium); the Agentschap voor Innovatie door Wetenschap en Technologie (IWT-Belgium); the Ministry of Education, Youth and Sports (MEYS) of the Czech Republic; the Council of Science and Industrial Research, India; the HOMING PLUS programme of the Foundation for Polish Science, cofinanced from European Union, Regional Development Fund; the OPUS programme of the National Science Center (Poland); the Compagnia di San Paolo (Torino); MIUR project 20108T4XTM (Italy); the Thalis and Aristeia programmes cofinanced by EU-ESF and the Greek NSRF; the National Priorities Research Program by Qatar National Research Fund; the Rachadapisek Sompot Fund for Postdoctoral Fellowship, Chulalongkorn University (Thailand); the Chulalongkorn Academic into Its 2nd Century Project Advancement Project (Thailand); and the Welch Foundation, contract C-1845.

## References

[1] J. D. Bjorken and E. A. Paschos, "Inelastic electron–proton and $\gamma$–proton scattering and the structure of the nucleon", *Phys. Rev.* **185** (1969) 1975, doi:10.1103/PhysRev.185.1975.

[2] CDF Collaboration, "Measurement of the lepton charge asymmetry in W boson decays produced in $p\overline{p}$ collisions", *Phys. Rev. Lett.* **81** (1998) 5754, doi:10.1103/PhysRevLett.81.5754, arXiv:hep-ex/9809001.

[3] CDF Collaboration, "Direct measurement of the W production charge asymmetry in $p\overline{p}$ Collisions at $\sqrt{s} = 1.96\,\text{TeV}$", *Phys. Rev. Lett.* **102** (2009) 181801, doi:10.1103/PhysRevLett.102.181801, arXiv:0901.2169.

[4] D0 Collaboration, "Measurement of the muon charge asymmetry from W boson decays", *Phys. Rev. D* **77** (2008) 011106, doi:10.1103/PhysRevD.77.011106, arXiv:0709.4254.

[5] D0 Collaboration, "Measurement of the electron charge asymmetry in $p\overline{p} \to W + X \to e\nu + X$ events at $\sqrt{s} = 1.96\,\text{TeV}$", *Phys. Rev. Lett.* **101** (2008) 211801, doi:10.1103/PhysRevLett.101.211801, arXiv:0807.3367.

[6] D0 Collaboration, "Measurement of the muon charge asymmetry in $p\overline{p} \to W + X \to \mu\nu + X$ events at $\sqrt{s} = 1.96\,\text{TeV}$", *Phys. Rev. D* **88** (2013) 091102, doi:10.1103/PhysRevD.88.091102, arXiv:1309.2591.

[7] CMS Collaboration, "Measurement of the lepton charge asymmetry in inclusive W production in pp collisions at $\sqrt{s} = 7\,\text{TeV}$", *JHEP* **04** (2011) 050, doi:10.1007/JHEP04(2011)050, arXiv:1103.3470.

[8] ATLAS Collaboration, "Measurement of the inclusive $W^{\pm}$ and $Z/\gamma$ cross sections in the e and $\mu$ decay channels in pp collisions at $\sqrt{s} = 7\,\text{TeV}$ with the ATLAS detector", *Phys. Rev. D* **85** (2012) 072004, doi:10.1103/PhysRevD.85.072004, arXiv:1109.5141.

[9] LHCb Collaboration, "Inclusive W and Z production in the forward region at $\sqrt{s} = 7\,\text{TeV}$", *JHEP* **06** (2012) 058, doi:10.1007/JHEP06(2012)058, arXiv:1204.1620.

[10] CMS Collaboration, "Measurement of the Electron Charge Asymmetry in Inclusive W Production in pp Collisions at $\sqrt{s} = 7\,\text{TeV}$", *Phys. Rev. Lett.* **109** (2012) 111806, doi:10.1103/PhysRevLett.109.111806, arXiv:1206.2598.

[11] CMS Collaboration, "Measurement of the muon charge asymmetry in inclusive $pp \to W + X$ production at $\sqrt{s} = 7$ TeV and an improved determination of light parton distribution functions", *Phys. Rev. D* **90** (2014) 032004, doi:10.1103/PhysRevD.90.032004, arXiv:1312.6283.

[12] CMS Collaboration, "The CMS experiment at the CERN LHC", *JINST* **3** (2008) S08004, doi:10.1088/1748-0221/3/08/S08004.

[13] S. Alioli, P. Nason, C. Oleari, and E. Re, "NLO vector-boson production matched with shower in POWHEG", *JHEP* **07** (2008) 060, doi:10.1088/1126-6708/2008/07/060, arXiv:0805.4802.

[14] P. Nason, "A new method for combining NLO QCD with shower Monte Carlo algorithms", *JHEP* **11** (2004) 040, doi:10.1088/1126-6708/2004/11/040, arXiv:hep-ph/0409146.

[15] S. Frixione, P. Nason, and C. Oleari, "Matching NLO QCD computations with parton shower simulations: the POWHEG method", *JHEP* **11** (2007) 070, doi:10.1088/1126-6708/2007/11/070, arXiv:0709.2092.

[16] S. Alioli, P. Nason, C. Oleari, and E. Re, "A general framework for implementing NLO calculations in shower Monte Carlo programs: the POWHEG BOX", *JHEP* **06** (2010) 043, doi:10.1007/JHEP06(2010)043, arXiv:1002.2581.

[17] T. Sjöstrand, S. Mrenna, and P. Skands, "PYTHIA 6.4 physics and manual", *JHEP* **05** (2006) 026, doi:10.1088/1126-6708/2006/05/026, arXiv:hep-ph/0603175.

[18] H.-L. Lai et al., "New parton distributions for collider physics", *Phys. Rev. D* **82** (2010) 074024, doi:10.1103/PhysRevD.82.074024, arXiv:1007.2241.

[19] N. Davidson et al., "Universal Interface of TAUOLA Technical and Physics Documentation", *Comput. Phys. Commun.* **183** (2012) 821, doi:10.1016/j.cpc.2011.12.009, arXiv:1002.0543.

[20] J. Pumplin et al., "New generation of parton distributions with uncertainties from global QCD analysis", *JHEP* **07** (2002) 012, doi:10.1088/1126-6708/2002/07/012, arXiv:hep-ph/0201195.

[21] GEANT4 Collaboration, "GEANT4—a simulation toolkit", *Nucl. Instrum. Meth. A* **506** (2003) 250, doi:10.1016/S0168-9002(03)01368-8.

[22] CMS Collaboration, "Measurement of the inelastic proton-proton cross section at $\sqrt{s} = 7$ TeV", *Phys. Lett. B* **722** (2013) 5, doi:10.1016/j.physletb.2013.03.024, arXiv:1210.6718.

[23] A. Bodek et al., "Extracting muon momentum scale corrections for hadron collider experiments", *Eur. Phys. J. C* **72** (2012) 2194, doi:10.1140/epjc/s10052-012-2194-8, arXiv:1208.3710.

[24] CMS Collaboration, "Measurements of inclusive W and Z cross sections in pp collisions at $\sqrt{s} = 7$ TeV with the CMS experiment", *JHEP* **10** (2011) 132, doi:10.1007/JHEP10(2011)132, arXiv:1107.4789.

[25] CMS Collaboration, "Performance of CMS muon reconstruction in pp collision events at $\sqrt{s} = 7\,\text{TeV}$", *JINST* **7** (2012) P10002, doi:10.1088/1748-0221/7/10/P10002, arXiv:1206.4071.

[26] CMS Collaboration, "Particle-flow event reconstruction in CMS and performance for jets, taus, and $E_{\text{T}}^{\text{miss}}$", CMS Physics Analysis Summary CMS-PAS-PFT-09-001, CERN, 2009.

[27] CMS Collaboration, "Commissioning of the particle-flow event reconstruction with the first LHC collisions recorded in the CMS detector", CMS Physics Analysis Summary CMS-PAS-PFT-10-001, CERN, 2010.

[28] CMS Collaboration, "Performance of the CMS missing transverse momentum reconstruction in pp data at $\sqrt{s} = 8\,\text{TeV}$", *JINST* **10** (2015) P02006, doi:10.1088/1748-0221/10/02/P02006, arXiv:1411.0511.

[29] D0 Collaboration, "A novel method for modeling the recoil in W boson events at hadron collider", *Nucl. Instrum. Meth. A* **609** (2009) 250, doi:10.1016/j.nima.2009.08.056, arXiv:0907.3713.

[30] CMS Collaboration, "Missing transverse energy performance of the CMS detector", *JINST* **6** (2011) P09001, doi:10.1088/1748-0221/6/09/P09001, arXiv:1106.5048.

[31] M. Czakon and A. Mitov, "Top++: a program for the calculation of the top-pair cross-section at hadron colliders", *Comput. Phys. Commun.* **185** (2014) 2930, doi:10.1016/j.cpc.2014.06.021, arXiv:1112.5675.

[32] Particle Data Group Collaboration, "Review of particle physics", *Chin. Phys. C* **38** (2014) 090001, doi:10.1088/1674-1137/38/9/090001.

[33] G. Nanava and Z. Was, "How to use SANC to improve the PHOTOS Monte Carlo simulation of bremsstrahlung in leptonic W boson decays", *Acta Phys. Polon. B* **34** (2003) 4561, arXiv:hep-ph/0303260.

[34] H. Burkhardt and B. Pietrzyk, "Update of the hadronic contribution to the QED vacuum polarization", *Phys. Lett. B* **513** (2001) 46, doi:10.1016/S0370-2693(01)00393-8.

[35] A. D. Martin, W. J. Stirling, R. S. Thorne, and G. Watt, "Parton distributions for the LHC", *Eur. Phys. J. C* **63** (2009) 189, doi:10.1140/epjc/s10052-009-1072-5, arXiv:0901.0002.

[36] NNPDF Collaboration, "Impact of heavy quark masses on parton distributions and LHC phenomenology", *Nucl. Phys. B* **849** (2011) 296, doi:10.1016/j.nuclphysb.2011.03.021, arXiv:1101.1300.

[37] CMS Collaboration, "CMS luminosity based on pixel cluster counting – Summer 2013 update", CMS Physics Analysis Summary CMS-PAS-LUM-13-001, CERN, 2013.

[38] Y. Li and F. Petriello, "Combining QCD and electroweak corrections to dilepton production in the framework of the FEWZ simulation code", *Phys. Rev. D* **86** (2012) 094034, doi:10.1103/PhysRevD.86.094034, arXiv:1208.5967.

[39] NNPDF Collaboration, "Parton distributions for the LHC Run II", *JHEP* **04** (2015) 040, doi:10.1007/JHEP04(2015)040, arXiv:1410.8849.

[40] H1 and ZEUS Collaborations, "Combination and QCD Analysis of the HERA Inclusive Cross Sections", in *Proc. of the 35th Int. Conf. of High Energy Physics*, volume 168. 2010. PoS(ICHEP2010)169. Grids available at `http://www.desy.de/h1zeus/combined_results/index.php?do=proton_structure`.

[41] L. A. Harland-Lang, A. D. Martin, P. Motylinski, and R. S. Thorne, "Parton distributions in the LHC era: MMHT 2014 PDFs", *Eur. Phys. J. C* **75** (2015) 204, `doi:10.1140/epjc/s10052-015-3397-6`, `arXiv:1412.3989`.

[42] S. Alekhin, J. Blumlein, and S. Moch, "The ABM parton distributions tuned to LHC data", *Phys. Rev. D* **89** (2014) 054028, `doi:10.1103/PhysRevD.89.054028`, `arXiv:1310.3059`.

[43] H1 and ZEUS Collaborations, "Combination of measurements of inclusive deep inelastic $e^{\pm}p$ scattering cross sections and QCD analysis of HERA data", *Eur. Phys. J. C* **75** (2015) 580, `doi:10.1140/epjc/s10052-015-3710-4`, `arXiv:1506.06042`.

[44] J. M. Campbell and R. K. Ellis, "Update on vector boson pair production at hadron colliders", *Phys. Rev. D* **60** (1999) 113006, `doi:10.1103/PhysRevD.60.113006`, `arXiv:hep-ph/9905386`.

[45] J. M. Campbell and R. K. Ellis, "MCFM for the Tevatron and the LHC", *Nucl. Phys. Proc. Suppl.* **205–206** (2010) 10, `doi:10.1016/j.nuclphysbps.2010.08.011`, `arXiv:1007.3492`.

[46] T. Carli et al., "A posteriori inclusion of parton density functions in NLO QCD final-state calculations at hadron colliders: the APPLGRID project", *Eur. Phys. J. C* **66** (2010) 503, `doi:10.1140/epjc/s10052-010-1255-0`, `arXiv:0911.2985`.

[47] S. Alekhin et al., "HERAFitter", *Eur. Phys. J. C* **75** (2015) 304, `doi:10.1140/epjc/s10052-015-3480-z`, `arXiv:1410.4412`.

[48] HERAFitter web site, `http://www.herafitter.org`.

[49] V. N. Gribov and L. N. Lipatov, "Deep inelastic e-p scattering in perturbation theory", *Sov. J. Nucl. Phys.* **15** (1972) 438.

[50] G. Altarelli and G. Parisi, "Asymptotic freedom in parton language", *Nucl. Phys. B* **126** (1977) 298, `doi:10.1016/0550-3213(77)90384-4`.

[51] G. Curci, W. Furmanski, and R. Petronzio, "Evolution of parton densities beyond leading order: The non-singlet case", *Nucl. Phys. B* **175** (1980) 27, `doi:10.1016/0550-3213(80)90003-6`.

[52] W. Furmanski and R. Petronzio, "Singlet parton densities beyond leading order", *Phys. Lett. B* **97** (1980) 437, `doi:10.1016/0370-2693(80)90636-X`.

[53] S. Moch, J. A. M. Vermaseren, and A. Vogt, "The three-loop splitting functions in QCD: the non-singlet case", *Nucl. Phys. B* **688** (2004) 101, `doi:10.1016/j.nuclphysb.2004.03.030`, `arXiv:hep-ph/0403192`.

[54] A. Vogt, S. Moch, and J. A. M. Vermaseren, "The three-loop splitting functions in QCD: the singlet case", *Nucl. Phys. B* **691** (2004) 129, `doi:10.1016/j.nuclphysb.2004.04.024`, `arXiv:hep-ph/0404111`.

[55] M. Botje, "QCDNUM: fast QCD evolution and convolution", *Comput. Phys. Commun.* **182** (2011) 490, doi:10.1016/j.cpc.2010.10.020, arXiv:1005.1481.

[56] R. S. Thorne, "Variable-flavor number scheme for NNLO", *Phys. Rev. D* **73** (2006) 054019, doi:10.1103/PhysRevD.73.054019, arXiv:hep-ph/0601245.

[57] H1 and ZEUS Collaborations, "Combined measurement and QCD analysis of the inclusive $e^{\pm}p$ scattering cross sections at HERA", *JHEP* **01** (2010) 109, doi:10.1007/JHEP01(2010)109, arXiv:0911.0884.

# A The CMS Collaboration

**Yerevan Physics Institute, Yerevan, Armenia**
V. Khachatryan, A.M. Sirunyan, A. Tumasyan

**Institut für Hochenergiephysik der OeAW, Wien, Austria**
W. Adam, E. Asilar, T. Bergauer, J. Brandstetter, E. Brondolin, M. Dragicevic, J. Erö, M. Flechl, M. Friedl, R. Frühwirth[1], V.M. Ghete, C. Hartl, N. Hörmann, J. Hrubec, M. Jeitler[1], A. König, M. Krammer[1], I. Krätschmer, D. Liko, T. Matsushita, I. Mikulec, D. Rabady, N. Rad, B. Rahbaran, H. Rohringer, J. Schieck[1], R. Schöfbeck, J. Strauss, W. Treberer-Treberspurg, W. Waltenberger, C.-E. Wulz[1]

**National Centre for Particle and High Energy Physics, Minsk, Belarus**
V. Mossolov, N. Shumeiko, J. Suarez Gonzalez

**Universiteit Antwerpen, Antwerpen, Belgium**
S. Alderweireldt, T. Cornelis, E.A. De Wolf, X. Janssen, A. Knutsson, J. Lauwers, S. Luyckx, M. Van De Klundert, H. Van Haevermaet, P. Van Mechelen, N. Van Remortel, A. Van Spilbeeck

**Vrije Universiteit Brussel, Brussel, Belgium**
S. Abu Zeid, F. Blekman, J. D'Hondt, N. Daci, I. De Bruyn, K. Deroover, N. Heracleous, J. Keaveney, S. Lowette, S. Moortgat, L. Moreels, A. Olbrechts, Q. Python, D. Strom, S. Tavernier, W. Van Doninck, P. Van Mulders, I. Van Parijs

**Université Libre de Bruxelles, Bruxelles, Belgium**
H. Brun, C. Caillol, B. Clerbaux, G. De Lentdecker, G. Fasanella, L. Favart, R. Goldouzian, A. Grebenyuk, G. Karapostoli, T. Lenzi, A. Léonard, T. Maerschalk, A. Marinov, A. Randleconde, T. Seva, C. Vander Velde, P. Vanlaer, R. Yonamine, F. Zenoni, F. Zhang[2]

**Ghent University, Ghent, Belgium**
L. Benucci, A. Cimmino, S. Crucy, D. Dobur, A. Fagot, G. Garcia, M. Gul, J. Mccartin, A.A. Ocampo Rios, D. Poyraz, D. Ryckbosch, S. Salva, M. Sigamani, M. Tytgat, W. Van Driessche, E. Yazgan, N. Zaganidis

**Université Catholique de Louvain, Louvain-la-Neuve, Belgium**
S. Basegmez, C. Beluffi[3], O. Bondu, S. Brochet, G. Bruno, A. Caudron, L. Ceard, S. De Visscher, C. Delaere, M. Delcourt, D. Favart, L. Forthomme, A. Giammanco, A. Jafari, P. Jez, M. Komm, V. Lemaitre, A. Mertens, M. Musich, C. Nuttens, K. Piotrzkowski, L. Quertenmont, M. Selvaggi, M. Vidal Marono

**Université de Mons, Mons, Belgium**
N. Beliy, G.H. Hammad

**Centro Brasileiro de Pesquisas Fisicas, Rio de Janeiro, Brazil**
W.L. Aldá Júnior, F.L. Alves, G.A. Alves, L. Brito, M. Correa Martins Junior, M. Hamer, C. Hensel, A. Moraes, M.E. Pol, P. Rebello Teles

**Universidade do Estado do Rio de Janeiro, Rio de Janeiro, Brazil**
E. Belchior Batista Das Chagas, W. Carvalho, J. Chinellato[4], A. Custódio, E.M. Da Costa, D. De Jesus Damiao, C. De Oliveira Martins, S. Fonseca De Souza, L.M. Huertas Guativa, H. Malbouisson, D. Matos Figueiredo, C. Mora Herrera, L. Mundim, H. Nogima, W.L. Prado Da Silva, A. Santoro, A. Sznajder, E.J. Tonelli Manganote[4], A. Vilela Pereira

**Universidade Estadual Paulista [a], Universidade Federal do ABC [b], São Paulo, Brazil**
S. Ahuja[a], C.A. Bernardes[b], A. De Souza Santos[b], S. Dogra[a], T.R. Fernandez Perez Tomei[a],

E.M. Gregores[b], P.G. Mercadante[b], C.S. Moon[a,5], S.F. Novaes[a], Sandra S. Padula[a], D. Romero Abad[b], J.C. Ruiz Vargas

**Institute for Nuclear Research and Nuclear Energy, Sofia, Bulgaria**
A. Aleksandrov, R. Hadjiiska, P. Iaydjiev, M. Rodozov, S. Stoykova, G. Sultanov, M. Vutova

**University of Sofia, Sofia, Bulgaria**
A. Dimitrov, I. Glushkov, L. Litov, B. Pavlov, P. Petkov

**Beihang University, Beijing, China**
W. Fang[6]

**Institute of High Energy Physics, Beijing, China**
M. Ahmad, J.G. Bian, G.M. Chen, H.S. Chen, M. Chen, T. Cheng, R. Du, C.H. Jiang, D. Leggat, R. Plestina[7], F. Romeo, S.M. Shaheen, A. Spiezia, J. Tao, C. Wang, Z. Wang, H. Zhang

**State Key Laboratory of Nuclear Physics and Technology, Peking University, Beijing, China**
C. Asawatangtrakuldee, Y. Ban, Q. Li, S. Liu, Y. Mao, S.J. Qian, D. Wang, Z. Xu

**Universidad de Los Andes, Bogota, Colombia**
C. Avila, A. Cabrera, L.F. Chaparro Sierra, C. Florez, J.P. Gomez, B. Gomez Moreno, J.C. Sanabria

**University of Split, Faculty of Electrical Engineering, Mechanical Engineering and Naval Architecture, Split, Croatia**
N. Godinovic, D. Lelas, I. Puljak, P.M. Ribeiro Cipriano

**University of Split, Faculty of Science, Split, Croatia**
Z. Antunovic, M. Kovac

**Institute Rudjer Boskovic, Zagreb, Croatia**
V. Brigljevic, K. Kadija, J. Luetic, S. Micanovic, L. Sudic

**University of Cyprus, Nicosia, Cyprus**
A. Attikis, G. Mavromanolakis, J. Mousa, C. Nicolaou, F. Ptochos, P.A. Razis, H. Rykaczewski

**Charles University, Prague, Czech Republic**
M. Finger[8], M. Finger Jr.[8]

**Universidad San Francisco de Quito, Quito, Ecuador**
E. Carrera Jarrin

**Academy of Scientific Research and Technology of the Arab Republic of Egypt, Egyptian Network of High Energy Physics, Cairo, Egypt**
A.A. Abdelalim[9,10], E. El-khateeb[11,11], T. Elkafrawy[11], M.A. Mahmoud[12,13]

**National Institute of Chemical Physics and Biophysics, Tallinn, Estonia**
B. Calpas, M. Kadastik, M. Murumaa, L. Perrini, M. Raidal, A. Tiko, C. Veelken

**Department of Physics, University of Helsinki, Helsinki, Finland**
P. Eerola, J. Pekkanen, M. Voutilainen

**Helsinki Institute of Physics, Helsinki, Finland**
J. Härkönen, V. Karimäki, R. Kinnunen, T. Lampén, K. Lassila-Perini, S. Lehti, T. Lindén, P. Luukka, T. Peltola, J. Tuominiemi, E. Tuovinen, L. Wendland

**Lappeenranta University of Technology, Lappeenranta, Finland**
J. Talvitie, T. Tuuva

**DSM/IRFU, CEA/Saclay, Gif-sur-Yvette, France**
M. Besancon, F. Couderc, M. Dejardin, D. Denegri, B. Fabbro, J.L. Faure, C. Favaro, F. Ferri, S. Ganjour, A. Givernaud, P. Gras, G. Hamel de Monchenault, P. Jarry, E. Locci, M. Machet, J. Malcles, J. Rander, A. Rosowsky, M. Titov, A. Zghiche

**Laboratoire Leprince-Ringuet, Ecole Polytechnique, IN2P3-CNRS, Palaiseau, France**
A. Abdulsalam, I. Antropov, S. Baffioni, F. Beaudette, P. Busson, L. Cadamuro, E. Chapon, C. Charlot, O. Davignon, R. Granier de Cassagnac, M. Jo, S. Lisniak, P. Miné, I.N. Naranjo, M. Nguyen, C. Ochando, G. Ortona, P. Paganini, P. Pigard, S. Regnard, R. Salerno, Y. Sirois, T. Strebler, Y. Yilmaz, A. Zabi

**Institut Pluridisciplinaire Hubert Curien, Université de Strasbourg, Université de Haute Alsace Mulhouse, CNRS/IN2P3, Strasbourg, France**
J.-L. Agram[14], J. Andrea, A. Aubin, D. Bloch, J.-M. Brom, M. Buttignol, E.C. Chabert, N. Chanon, C. Collard, E. Conte[14], X. Coubez, J.-C. Fontaine[14], D. Gelé, U. Goerlach, C. Goetzmann, A.-C. Le Bihan, J.A. Merlin[15], K. Skovpen, P. Van Hove

**Centre de Calcul de l'Institut National de Physique Nucleaire et de Physique des Particules, CNRS/IN2P3, Villeurbanne, France**
S. Gadrat

**Université de Lyon, Université Claude Bernard Lyon 1, CNRS-IN2P3, Institut de Physique Nucléaire de Lyon, Villeurbanne, France**
S. Beauceron, C. Bernet, G. Boudoul, E. Bouvier, C.A. Carrillo Montoya, R. Chierici, D. Contardo, B. Courbon, P. Depasse, H. El Mamouni, J. Fan, J. Fay, S. Gascon, M. Gouzevitch, B. Ille, F. Lagarde, I.B. Laktineh, M. Lethuillier, L. Mirabito, A.L. Pequegnot, S. Perries, A. Popov[16], J.D. Ruiz Alvarez, D. Sabes, V. Sordini, M. Vander Donckt, P. Verdier, S. Viret

**Georgian Technical University, Tbilisi, Georgia**
T. Toriashvili[17]

**Tbilisi State University, Tbilisi, Georgia**
D. Lomidze

**RWTH Aachen University, I. Physikalisches Institut, Aachen, Germany**
C. Autermann, S. Beranek, L. Feld, A. Heister, M.K. Kiesel, K. Klein, M. Lipinski, A. Ostapchuk, M. Preuten, F. Raupach, S. Schael, J.F. Schulte, T. Verlage, H. Weber, V. Zhukov[16]

**RWTH Aachen University, III. Physikalisches Institut A, Aachen, Germany**
M. Ata, M. Brodski, E. Dietz-Laursonn, D. Duchardt, M. Endres, M. Erdmann, S. Erdweg, T. Esch, R. Fischer, A. Güth, T. Hebbeker, C. Heidemann, K. Hoepfner, S. Knutzen, M. Merschmeyer, A. Meyer, P. Millet, S. Mukherjee, M. Olschewski, K. Padeken, P. Papacz, T. Pook, M. Radziej, H. Reithler, M. Rieger, F. Scheuch, L. Sonnenschein, D. Teyssier, S. Thüer

**RWTH Aachen University, III. Physikalisches Institut B, Aachen, Germany**
V. Cherepanov, Y. Erdogan, G. Flügge, H. Geenen, M. Geisler, F. Hoehle, B. Kargoll, T. Kress, A. Künsken, J. Lingemann, A. Nehrkorn, A. Nowack, I.M. Nugent, C. Pistone, O. Pooth, A. Stahl[15]

**Deutsches Elektronen-Synchrotron, Hamburg, Germany**
M. Aldaya Martin, I. Asin, K. Beernaert, O. Behnke, U. Behrens, K. Borras[18], A. Burgmeier, A. Campbell, C. Contreras-Campana, F. Costanza, C. Diez Pardos, G. Dolinska, S. Dooling, G. Eckerlin, D. Eckstein, T. Eichhorn, E. Eren, E. Gallo[19], J. Garay Garcia, A. Geiser, A. Gizhko, P. Gunnellini, J. Hauk, M. Hempel[20], H. Jung, A. Kalogeropoulos, O. Karacheban[20],

M. Kasemann, P. Katsas, J. Kieseler, C. Kleinwort, I. Korol, W. Lange, J. Leonard, K. Lipka, A. Lobanov, W. Lohmann[20], R. Mankel, I.-A. Melzer-Pellmann, A.B. Meyer, G. Mittag, J. Mnich, A. Mussgiller, A. Nayak, E. Ntomari, D. Pitzl, R. Placakyte, A. Raspereza, B. Roland, M.Ö. Sahin, P. Saxena, T. Schoerner-Sadenius, C. Seitz, S. Spannagel, N. Stefaniuk, K.D. Trippkewitz, G.P. Van Onsem, R. Walsh, C. Wissing

**University of Hamburg, Hamburg, Germany**
V. Blobel, M. Centis Vignali, A.R. Draeger, T. Dreyer, J. Erfle, E. Garutti, K. Goebel, D. Gonzalez, M. Görner, J. Haller, M. Hoffmann, R.S. Höing, A. Junkes, R. Klanner, R. Kogler, N. Kovalchuk, T. Lapsien, T. Lenz, I. Marchesini, D. Marconi, M. Meyer, M. Niedziela, D. Nowatschin, J. Ott, F. Pantaleo[15], T. Peiffer, A. Perieanu, N. Pietsch, J. Poehlsen, C. Sander, C. Scharf, P. Schleper, E. Schlieckau, A. Schmidt, S. Schumann, J. Schwandt, H. Stadie, G. Steinbrück, F.M. Stober, H. Tholen, D. Troendle, E. Usai, L. Vanelderen, A. Vanhoefer, B. Vormwald

**Institut für Experimentelle Kernphysik, Karlsruhe, Germany**
C. Barth, C. Baus, J. Berger, C. Böser, E. Butz, T. Chwalek, F. Colombo, W. De Boer, A. Descroix, A. Dierlamm, S. Fink, F. Frensch, R. Friese, M. Giffels, A. Gilbert, D. Haitz, F. Hartmann[15], S.M. Heindl, U. Husemann, I. Katkov[16], A. Kornmayer[15], P. Lobelle Pardo, B. Maier, H. Mildner, M.U. Mozer, T. Müller, Th. Müller, M. Plagge, G. Quast, K. Rabbertz, S. Röcker, F. Roscher, M. Schröder, G. Sieber, H.J. Simonis, R. Ulrich, J. Wagner-Kuhr, S. Wayand, M. Weber, T. Weiler, S. Williamson, C. Wöhrmann, R. Wolf

**Institute of Nuclear and Particle Physics (INPP), NCSR Demokritos, Aghia Paraskevi, Greece**
G. Anagnostou, G. Daskalakis, T. Geralis, V.A. Giakoumopoulou, A. Kyriakis, D. Loukas, A. Psallidas, I. Topsis-Giotis

**National and Kapodistrian University of Athens, Athens, Greece**
A. Agapitos, S. Kesisoglou, A. Panagiotou, N. Saoulidou, E. Tziaferi

**University of Ioánnina, Ioánnina, Greece**
I. Evangelou, G. Flouris, C. Foudas, P. Kokkas, N. Loukas, N. Manthos, I. Papadopoulos, E. Paradas, J. Strologas

**MTA-ELTE Lendület CMS Particle and Nuclear Physics Group**
N. Filipovic

**Wigner Research Centre for Physics, Budapest, Hungary**
G. Bencze, C. Hajdu, P. Hidas, D. Horvath[21], F. Sikler, V. Veszpremi, G. Vesztergombi[22], A.J. Zsigmond

**Institute of Nuclear Research ATOMKI, Debrecen, Hungary**
N. Beni, S. Czellar, J. Karancsi[23], J. Molnar, Z. Szillasi

**University of Debrecen, Debrecen, Hungary**
M. Bartók[22], A. Makovec, P. Raics, Z.L. Trocsanyi, B. Ujvari

**National Institute of Science Education and Research, Bhubaneswar, India**
S. Choudhury[24], P. Mal, K. Mandal, D.K. Sahoo, N. Sahoo, S.K. Swain

**Panjab University, Chandigarh, India**
S. Bansal, S.B. Beri, V. Bhatnagar, R. Chawla, R. Gupta, U.Bhawandeep, A.K. Kalsi, A. Kaur, M. Kaur, R. Kumar, A. Mehta, M. Mittal, J.B. Singh, G. Walia

**University of Delhi, Delhi, India**
Ashok Kumar, A. Bhardwaj, B.C. Choudhary, R.B. Garg, S. Keshri, A. Kumar, S. Malhotra, M. Naimuddin, N. Nishu, K. Ranjan, R. Sharma, V. Sharma

**Saha Institute of Nuclear Physics, Kolkata, India**
R. Bhattacharya, S. Bhattacharya, K. Chatterjee, S. Dey, S. Dutta, S. Ghosh, N. Majumdar, A. Modak, K. Mondal, S. Mukhopadhyay, S. Nandan, A. Purohit, A. Roy, D. Roy, S. Roy Chowdhury, S. Sarkar, M. Sharan

**Bhabha Atomic Research Centre, Mumbai, India**
R. Chudasama, D. Dutta, V. Jha, V. Kumar, A.K. Mohanty[15], L.M. Pant, P. Shukla, A. Topkar

**Tata Institute of Fundamental Research, Mumbai, India**
T. Aziz, S. Banerjee, S. Bhowmik[25], R.M. Chatterjee, R.K. Dewanjee, S. Dugad, S. Ganguly, S. Ghosh, M. Guchait, A. Gurtu[26], Sa. Jain, G. Kole, S. Kumar, B. Mahakud, M. Maity[25], G. Majumder, K. Mazumdar, S. Mitra, G.B. Mohanty, B. Parida, T. Sarkar[25], N. Sur, B. Sutar, N. Wickramage[27]

**Indian Institute of Science Education and Research (IISER), Pune, India**
S. Chauhan, S. Dube, A. Kapoor, K. Kothekar, A. Rane, S. Sharma

**Institute for Research in Fundamental Sciences (IPM), Tehran, Iran**
H. Bakhshiansohi, H. Behnamian, S.M. Etesami[28], A. Fahim[29], M. Khakzad, M. Mohammadi Najafabadi, M. Naseri, S. Paktinat Mehdiabadi, F. Rezaei Hosseinabadi, B. Safarzadeh[30], M. Zeinali

**University College Dublin, Dublin, Ireland**
M. Felcini, M. Grunewald

**INFN Sezione di Bari [a], Università di Bari [b], Politecnico di Bari [c], Bari, Italy**
M. Abbrescia[a,b], C. Calabria[a,b], C. Caputo[a,b], A. Colaleo[a], D. Creanza[a,c], L. Cristella[a,b], N. De Filippis[a,c], M. De Palma[a,b], L. Fiore[a], G. Iaselli[a,c], G. Maggi[a,c], M. Maggi[a], G. Miniello[a,b], S. My[a,b], S. Nuzzo[a,b], A. Pompili[a,b], G. Pugliese[a,c], R. Radogna[a,b], A. Ranieri[a], G. Selvaggi[a,b], L. Silvestris[a,15], R. Venditti[a,b]

**INFN Sezione di Bologna [a], Università di Bologna [b], Bologna, Italy**
G. Abbiendi[a], C. Battilana[15], D. Bonacorsi[a,b], S. Braibant-Giacomelli[a,b], L. Brigliadori[a,b], R. Campanini[a,b], P. Capiluppi[a,b], A. Castro[a,b], F.R. Cavallo[a], S.S. Chhibra[a,b], G. Codispoti[a,b], M. Cuffiani[a,b], G.M. Dallavalle[a], F. Fabbri[a], A. Fanfani[a,b], D. Fasanella[a,b], P. Giacomelli[a], C. Grandi[a], L. Guiducci[a,b], S. Marcellini[a], G. Masetti[a], A. Montanari[a], F.L. Navarria[a,b], A. Perrotta[a], A.M. Rossi[a,b], T. Rovelli[a,b], G.P. Siroli[a,b], N. Tosi[a,b,15]

**INFN Sezione di Catania [a], Università di Catania [b], Catania, Italy**
G. Cappello[b], M. Chiorboli[a,b], S. Costa[a,b], A. Di Mattia[a], F. Giordano[a,b], R. Potenza[a,b], A. Tricomi[a,b], C. Tuve[a,b]

**INFN Sezione di Firenze [a], Università di Firenze [b], Firenze, Italy**
G. Barbagli[a], V. Ciulli[a,b], C. Civinini[a], R. D'Alessandro[a,b], E. Focardi[a,b], V. Gori[a,b], P. Lenzi[a,b], M. Meschini[a], S. Paoletti[a], G. Sguazzoni[a], L. Viliani[a,b,15]

**INFN Laboratori Nazionali di Frascati, Frascati, Italy**
L. Benussi, S. Bianco, F. Fabbri, D. Piccolo, F. Primavera[15]

**INFN Sezione di Genova [a], Università di Genova [b], Genova, Italy**
V. Calvelli[a,b], F. Ferro[a], M. Lo Vetere[a,b], M.R. Monge[a,b], E. Robutti[a], S. Tosi[a,b]

**INFN Sezione di Milano-Bicocca [a], Università di Milano-Bicocca [b], Milano, Italy**
L. Brianza, M.E. Dinardo[a,b], S. Fiorendi[a,b], S. Gennai[a], R. Gerosa[a,b], A. Ghezzi[a,b], P. Govoni[a,b], S. Malvezzi[a], R.A. Manzoni[a,b,15], B. Marzocchi[a,b], D. Menasce[a], L. Moroni[a], M. Paganoni[a,b], D. Pedrini[a], S. Pigazzini, S. Ragazzi[a,b], N. Redaelli[a], T. Tabarelli de Fatis[a,b]

**INFN Sezione di Napoli [a], Università di Napoli 'Federico II' [b], Napoli, Italy, Università della Basilicata [c], Potenza, Italy, Università G. Marconi [d], Roma, Italy**
S. Buontempo[a], N. Cavallo[a,c], S. Di Guida[a,d,15], M. Esposito[a,b], F. Fabozzi[a,c], A.O.M. Iorio[a,b], G. Lanza[a], L. Lista[a], S. Meola[a,d,15], M. Merola[a], P. Paolucci[a,15], C. Sciacca[a,b], F. Thyssen

**INFN Sezione di Padova [a], Università di Padova [b], Padova, Italy, Università di Trento [c], Trento, Italy**
P. Azzi[a,15], N. Bacchetta[a], L. Benato[a,b], D. Bisello[a,b], A. Boletti[a,b], A. Branca[a,b], R. Carlin[a,b], P. Checchia[a], M. Dall'Osso[a,b,15], T. Dorigo[a], U. Dosselli[a], F. Gasparini[a,b], U. Gasparini[a,b], F. Gonella[a], A. Gozzelino[a], K. Kanishchev[a,c], S. Lacaprara[a], M. Margoni[a,b], A.T. Meneguzzo[a,b], J. Pazzini[a,b,15], N. Pozzobon[a,b], P. Ronchese[a,b], F. Simonetto[a,b], E. Torassa[a], M. Tosi[a,b], M. Zanetti, P. Zotto[a,b], A. Zucchetta[a,b,15], G. Zumerle[a,b]

**INFN Sezione di Pavia [a], Università di Pavia [b], Pavia, Italy**
A. Braghieri[a], A. Magnani[a,b], P. Montagna[a,b], S.P. Ratti[a,b], V. Re[a], C. Riccardi[a,b], P. Salvini[a], I. Vai[a,b], P. Vitulo[a,b]

**INFN Sezione di Perugia [a], Università di Perugia [b], Perugia, Italy**
L. Alunni Solestizi[a,b], G.M. Bilei[a], D. Ciangottini[a,b], L. Fanò[a,b], P. Lariccia[a,b], R. Leonardi[a,b], G. Mantovani[a,b], M. Menichelli[a], A. Saha[a], A. Santocchia[a,b]

**INFN Sezione di Pisa [a], Università di Pisa [b], Scuola Normale Superiore di Pisa [c], Pisa, Italy**
K. Androsov[a,31], P. Azzurri[a,15], G. Bagliesi[a], J. Bernardini[a], T. Boccali[a], R. Castaldi[a], M.A. Ciocci[a,31], R. Dell'Orso[a], S. Donato[a,c], G. Fedi, L. Foà[a,c†], A. Giassi[a], M.T. Grippo[a,31], F. Ligabue[a,c], T. Lomtadze[a], L. Martini[a,b], A. Messineo[a,b], F. Palla[a], A. Rizzi[a,b], A. Savoy-Navarro[a,32], P. Spagnolo[a], R. Tenchini[a], G. Tonelli[a,b], A. Venturi[a], P.G. Verdini[a]

**INFN Sezione di Roma [a], Università di Roma [b], Roma, Italy**
L. Barone[a,b], F. Cavallari[a], G. D'imperio[a,b,15], D. Del Re[a,b,15], M. Diemoz[a], S. Gelli[a,b], C. Jorda[a], E. Longo[a,b], F. Margaroli[a,b], P. Meridiani[a], G. Organtini[a,b], R. Paramatti[a], F. Preiato[a,b], S. Rahatlou[a,b], C. Rovelli[a], F. Santanastasio[a,b]

**INFN Sezione di Torino [a], Università di Torino [b], Torino, Italy, Università del Piemonte Orientale [c], Novara, Italy**
N. Amapane[a,b], R. Arcidiacono[a,c,15], S. Argiro[a,b], M. Arneodo[a,c], N. Bartosik[a], R. Bellan[a,b], C. Biino[a], N. Cartiglia[a], M. Costa[a,b], R. Covarelli[a,b], A. Degano[a,b], N. Demaria[a], L. Finco[a,b], B. Kiani[a,b], C. Mariotti[a], S. Maselli[a], E. Migliore[a,b], V. Monaco[a,b], E. Monteil[a,b], M.M. Obertino[a,b], L. Pacher[a,b], N. Pastrone[a], M. Pelliccioni[a], G.L. Pinna Angioni[a,b], F. Ravera[a,b], A. Romero[a,b], M. Ruspa[a,c], R. Sacchi[a,b], V. Sola[a], A. Solano[a,b], A. Staiano[a]

**INFN Sezione di Trieste [a], Università di Trieste [b], Trieste, Italy**
S. Belforte[a], V. Candelise[a,b], M. Casarsa[a], F. Cossutti[a], G. Della Ricca[a,b], B. Gobbo[a], C. La Licata[a,b], A. Schizzi[a,b], A. Zanetti[a]

**Kangwon National University, Chunchon, Korea**
S.K. Nam

**Kyungpook National University, Daegu, Korea**
D.H. Kim, G.N. Kim, M.S. Kim, D.J. Kong, S. Lee, S.W. Lee, Y.D. Oh, A. Sakharov, D.C. Son

**Chonbuk National University, Jeonju, Korea**
J.A. Brochero Cifuentes, H. Kim, T.J. Kim[33]

**Chonnam National University, Institute for Universe and Elementary Particles, Kwangju, Korea**
S. Song

**Korea University, Seoul, Korea**
S. Cho, S. Choi, Y. Go, D. Gyun, B. Hong, Y. Kim, B. Lee, K. Lee, K.S. Lee, S. Lee, J. Lim, S.K. Park, Y. Roh

**Seoul National University, Seoul, Korea**
H.D. Yoo

**University of Seoul, Seoul, Korea**
M. Choi, H. Kim, H. Kim, J.H. Kim, J.S.H. Lee, I.C. Park, G. Ryu, M.S. Ryu

**Sungkyunkwan University, Suwon, Korea**
Y. Choi, J. Goh, D. Kim, E. Kwon, J. Lee, I. Yu

**Vilnius University, Vilnius, Lithuania**
V. Dudenas, A. Juodagalvis, J. Vaitkus

**National Centre for Particle Physics, Universiti Malaya, Kuala Lumpur, Malaysia**
I. Ahmed, Z.A. Ibrahim, J.R. Komaragiri, M.A.B. Md Ali[34], F. Mohamad Idris[35], W.A.T. Wan Abdullah, M.N. Yusli, Z. Zolkapli

**Centro de Investigacion y de Estudios Avanzados del IPN, Mexico City, Mexico**
E. Casimiro Linares, H. Castilla-Valdez, E. De La Cruz-Burelo, I. Heredia-De La Cruz[36], A. Hernandez-Almada, R. Lopez-Fernandez, J. Mejia Guisao, A. Sanchez-Hernandez

**Universidad Iberoamericana, Mexico City, Mexico**
S. Carrillo Moreno, F. Vazquez Valencia

**Benemerita Universidad Autonoma de Puebla, Puebla, Mexico**
I. Pedraza, H.A. Salazar Ibarguen, C. Uribe Estrada

**Universidad Autónoma de San Luis Potosí, San Luis Potosí, Mexico**
A. Morelos Pineda

**University of Auckland, Auckland, New Zealand**
D. Krofcheck

**University of Canterbury, Christchurch, New Zealand**
P.H. Butler

**National Centre for Physics, Quaid-I-Azam University, Islamabad, Pakistan**
A. Ahmad, M. Ahmad, Q. Hassan, H.R. Hoorani, W.A. Khan, S. Qazi, M. Shoaib, M. Waqas

**National Centre for Nuclear Research, Swierk, Poland**
H. Bialkowska, M. Bluj, B. Boimska, T. Frueboes, M. Górski, M. Kazana, K. Nawrocki, K. Romanowska-Rybinska, M. Szleper, P. Traczyk, P. Zalewski

**Institute of Experimental Physics, Faculty of Physics, University of Warsaw, Warsaw, Poland**
G. Brona, K. Bunkowski, A. Byszuk[37], K. Doroba, A. Kalinowski, M. Konecki, J. Krolikowski, M. Misiura, M. Olszewski, M. Walczak

**Laboratório de Instrumentação e Física Experimental de Partículas, Lisboa, Portugal**
P. Bargassa, C. Beirão Da Cruz E Silva, A. Di Francesco, P. Faccioli, P.G. Ferreira Parracho, M. Gallinaro, J. Hollar, N. Leonardo, L. Lloret Iglesias, M.V. Nemallapudi, F. Nguyen, J. Rodrigues Antunes, J. Seixas, O. Toldaiev, D. Vadruccio, J. Varela, P. Vischia

**Joint Institute for Nuclear Research, Dubna, Russia**
I. Golutvin, A. Kamenev, V. Karjavin, V. Korenkov, G. Kozlov, A. Lanev, A. Malakhov, V. Matveev[38,39], V.V. Mitsyn, P. Moisenz, V. Palichik, V. Perelygin, S. Shmatov, S. Shulha, N. Skatchkov, V. Smirnov, E. Tikhonenko, N. Voytishin, A. Zarubin

**Petersburg Nuclear Physics Institute, Gatchina (St. Petersburg), Russia**
V. Golovtsov, Y. Ivanov, V. Kim[40], E. Kuznetsova[41], P. Levchenko, V. Murzin, V. Oreshkin, I. Smirnov, V. Sulimov, L. Uvarov, S. Vavilov, A. Vorobyev

**Institute for Nuclear Research, Moscow, Russia**
Yu. Andreev, A. Dermenev, S. Gninenko, N. Golubev, A. Karneyeu, M. Kirsanov, N. Krasnikov, A. Pashenkov, D. Tlisov, A. Toropin

**Institute for Theoretical and Experimental Physics, Moscow, Russia**
V. Epshteyn, V. Gavrilov, N. Lychkovskaya, V. Popov, I. Pozdnyakov, G. Safronov, A. Spiridonov, M. Toms, E. Vlasov, A. Zhokin

**National Research Nuclear University 'Moscow Engineering Physics Institute' (MEPhI), Moscow, Russia**
M. Chadeeva, R. Chistov, M. Danilov, O. Markin, E. Tarkovskii

**P.N. Lebedev Physical Institute, Moscow, Russia**
V. Andreev, M. Azarkin[39], I. Dremin[39], M. Kirakosyan, A. Leonidov[39], G. Mesyats, S.V. Rusakov

**Skobeltsyn Institute of Nuclear Physics, Lomonosov Moscow State University, Moscow, Russia**
A. Baskakov, A. Belyaev, E. Boos, V. Bunichev, M. Dubinin[42], L. Dudko, A. Gribushin, V. Klyukhin, O. Kodolova, I. Lokhtin, I. Miagkov, S. Obraztsov, S. Petrushanko, V. Savrin, A. Snigirev

**State Research Center of Russian Federation, Institute for High Energy Physics, Protvino, Russia**
I. Azhgirey, I. Bayshev, S. Bitioukov, V. Kachanov, A. Kalinin, D. Konstantinov, V. Krychkine, V. Petrov, R. Ryutin, A. Sobol, L. Tourtchanovitch, S. Troshin, N. Tyurin, A. Uzunian, A. Volkov

**University of Belgrade, Faculty of Physics and Vinca Institute of Nuclear Sciences, Belgrade, Serbia**
P. Adzic[43], P. Cirkovic, D. Devetak, J. Milosevic, V. Rekovic

**Centro de Investigaciones Energéticas Medioambientales y Tecnológicas (CIEMAT), Madrid, Spain**
J. Alcaraz Maestre, E. Calvo, M. Cerrada, M. Chamizo Llatas, N. Colino, B. De La Cruz, A. Delgado Peris, A. Escalante Del Valle, C. Fernandez Bedoya, J.P. Fernández Ramos, J. Flix, M.C. Fouz, P. Garcia-Abia, O. Gonzalez Lopez, S. Goy Lopez, J.M. Hernandez, M.I. Josa, E. Navarro De Martino, A. Pérez-Calero Yzquierdo, J. Puerta Pelayo, A. Quintario Olmeda, I. Redondo, L. Romero, M.S. Soares

**Universidad Autónoma de Madrid, Madrid, Spain**
J.F. de Trocóniz, M. Missiroli, D. Moran

**Universidad de Oviedo, Oviedo, Spain**
J. Cuevas, J. Fernandez Menendez, S. Folgueras, I. Gonzalez Caballero, E. Palencia Cortezon[15], J.M. Vizan Garcia

**Instituto de Física de Cantabria (IFCA), CSIC-Universidad de Cantabria, Santander, Spain**
I.J. Cabrillo, A. Calderon, J.R. Castiñeiras De Saa, E. Curras, P. De Castro Manzano, M. Fernandez, J. Garcia-Ferrero, G. Gomez, A. Lopez Virto, J. Marco, R. Marco, C. Martinez Rivero, F. Matorras, J. Piedra Gomez, T. Rodrigo, A.Y. Rodríguez-Marrero, A. Ruiz-Jimeno, L. Scodellaro, N. Trevisani, I. Vila, R. Vilar Cortabitarte

**CERN, European Organization for Nuclear Research, Geneva, Switzerland**
D. Abbaneo, E. Auffray, G. Auzinger, M. Bachtis, P. Baillon, A.H. Ball, D. Barney, A. Benaglia, L. Benhabib, G.M. Berruti, P. Bloch, A. Bocci, A. Bonato, C. Botta, H. Breuker, T. Camporesi, R. Castello, M. Cepeda, G. Cerminara, M. D'Alfonso, D. d'Enterria, A. Dabrowski, V. Daponte, A. David, M. De Gruttola, F. De Guio, A. De Roeck, E. Di Marco[44], M. Dobson, M. Dordevic, B. Dorney, T. du Pree, D. Duggan, M. Dünser, N. Dupont, A. Elliott-Peisert, G. Franzoni, J. Fulcher, W. Funk, D. Gigi, K. Gill, M. Girone, F. Glege, R. Guida, S. Gundacker, M. Guthoff, J. Hammer, P. Harris, J. Hegeman, V. Innocente, P. Janot, H. Kirschenmann, V. Knünz, M.J. Kortelainen, K. Kousouris, P. Lecoq, C. Lourenço, M.T. Lucchini, N. Magini, L. Malgeri, M. Mannelli, A. Martelli, L. Masetti, F. Meijers, S. Mersi, E. Meschi, F. Moortgat, S. Morovic, M. Mulders, H. Neugebauer, S. Orfanelli[45], L. Orsini, L. Pape, E. Perez, M. Peruzzi, A. Petrilli, G. Petrucciani, A. Pfeiffer, M. Pierini, D. Piparo, A. Racz, T. Reis, G. Rolandi[46], M. Rovere, M. Ruan, H. Sakulin, J.B. Sauvan, C. Schäfer, C. Schwick, M. Seidel, A. Sharma, P. Silva, M. Simon, P. Sphicas[47], J. Steggemann, M. Stoye, Y. Takahashi, D. Treille, A. Triossi, A. Tsirou, V. Veckalns[48], G.I. Veres[22], N. Wardle, H.K. Wöhri, A. Zagozdzinska[37], W.D. Zeuner

**Paul Scherrer Institut, Villigen, Switzerland**
W. Bertl, K. Deiters, W. Erdmann, R. Horisberger, Q. Ingram, H.C. Kaestli, D. Kotlinski, U. Langenegger, T. Rohe

**Institute for Particle Physics, ETH Zurich, Zurich, Switzerland**
F. Bachmair, L. Bäni, L. Bianchini, B. Casal, G. Dissertori, M. Dittmar, M. Donegà, P. Eller, C. Grab, C. Heidegger, D. Hits, J. Hoss, G. Kasieczka, P. Lecomte[†], W. Lustermann, B. Mangano, M. Marionneau, P. Martinez Ruiz del Arbol, M. Masciovecchio, M.T. Meinhard, D. Meister, F. Micheli, P. Musella, F. Nessi-Tedaldi, F. Pandolfi, J. Pata, F. Pauss, G. Perrin, L. Perrozzi, M. Quittnat, M. Rossini, M. Schönenberger, A. Starodumov[49], M. Takahashi, V.R. Tavolaro, K. Theofilatos, R. Wallny

**Universität Zürich, Zurich, Switzerland**
T.K. Aarrestad, C. Amsler[50], L. Caminada, M.F. Canelli, V. Chiochia, A. De Cosa, C. Galloni, A. Hinzmann, T. Hreus, B. Kilminster, C. Lange, J. Ngadiuba, D. Pinna, G. Rauco, P. Robmann, D. Salerno, Y. Yang

**National Central University, Chung-Li, Taiwan**
K.H. Chen, T.H. Doan, Sh. Jain, R. Khurana, M. Konyushikhin, C.M. Kuo, W. Lin, Y.J. Lu, A. Pozdnyakov, S.S. Yu

**National Taiwan University (NTU), Taipei, Taiwan**
Arun Kumar, P. Chang, Y.H. Chang, Y.W. Chang, Y. Chao, K.F. Chen, P.H. Chen, C. Dietz, F. Fiori, U. Grundler, W.-S. Hou, Y. Hsiung, Y.F. Liu, R.-S. Lu, M. Miñano Moya, E. Petrakou, J.f. Tsai, Y.M. Tzeng

**Chulalongkorn University, Faculty of Science, Department of Physics, Bangkok, Thailand**
B. Asavapibhop, K. Kovitanggoon, G. Singh, N. Srimanobhas, N. Suwonjandee

**Cukurova University, Adana, Turkey**
A. Adiguzel, S. Cerci[51], S. Damarseckin, Z.S. Demiroglu, C. Dozen, I. Dumanoglu, S. Girgis, G. Gokbulut, Y. Guler, E. Gurpinar, I. Hos, E.E. Kangal[52], A. Kayis Topaksu, G. Onengut[53], K. Ozdemir[54], S. Ozturk[55], B. Tali[51], H. Topakli[55], C. Zorbilmez

**Middle East Technical University, Physics Department, Ankara, Turkey**
B. Bilin, S. Bilmis, B. Isildak[56], G. Karapinar[57], M. Yalvac, M. Zeyrek

**Bogazici University, Istanbul, Turkey**
E. Gülmez, M. Kaya[58], O. Kaya[59], E.A. Yetkin[60], T. Yetkin[61]

**Istanbul Technical University, Istanbul, Turkey**
A. Cakir, K. Cankocak, S. Sen[62]

**Institute for Scintillation Materials of National Academy of Science of Ukraine, Kharkov, Ukraine**
B. Grynyov

**National Scientific Center, Kharkov Institute of Physics and Technology, Kharkov, Ukraine**
L. Levchuk, P. Sorokin

**University of Bristol, Bristol, United Kingdom**
R. Aggleton, F. Ball, L. Beck, J.J. Brooke, D. Burns, E. Clement, D. Cussans, H. Flacher, J. Goldstein, M. Grimes, G.P. Heath, H.F. Heath, J. Jacob, L. Kreczko, C. Lucas, Z. Meng, D.M. Newbold[63], S. Paramesvaran, A. Poll, T. Sakuma, S. Seif El Nasr-storey, S. Senkin, D. Smith, V.J. Smith

**Rutherford Appleton Laboratory, Didcot, United Kingdom**
K.W. Bell, A. Belyaev[64], C. Brew, R.M. Brown, L. Calligaris, D. Cieri, D.J.A. Cockerill, J.A. Coughlan, K. Harder, S. Harper, E. Olaiya, D. Petyt, C.H. Shepherd-Themistocleous, A. Thea, I.R. Tomalin, T. Williams, S.D. Worm

**Imperial College, London, United Kingdom**
M. Baber, R. Bainbridge, O. Buchmuller, A. Bundock, D. Burton, S. Casasso, M. Citron, D. Colling, L. Corpe, P. Dauncey, G. Davies, A. De Wit, M. Della Negra, P. Dunne, A. Elwood, D. Futyan, Y. Haddad, G. Hall, G. Iles, R. Lane, R. Lucas[63], L. Lyons, A.-M. Magnan, S. Malik, L. Mastrolorenzo, J. Nash, A. Nikitenko[49], J. Pela, B. Penning, M. Pesaresi, D.M. Raymond, A. Richards, A. Rose, C. Seez, A. Tapper, K. Uchida, M. Vazquez Acosta[65], T. Virdee[15], S.C. Zenz

**Brunel University, Uxbridge, United Kingdom**
J.E. Cole, P.R. Hobson, A. Khan, P. Kyberd, D. Leslie, I.D. Reid, P. Symonds, L. Teodorescu, M. Turner

**Baylor University, Waco, USA**
A. Borzou, K. Call, J. Dittmann, K. Hatakeyama, H. Liu, N. Pastika

**The University of Alabama, Tuscaloosa, USA**
O. Charaf, S.I. Cooper, C. Henderson, P. Rumerio

**Boston University, Boston, USA**
D. Arcaro, A. Avetisyan, T. Bose, D. Gastler, D. Rankin, C. Richardson, J. Rohlf, L. Sulak, D. Zou

**Brown University, Providence, USA**
J. Alimena, G. Benelli, E. Berry, D. Cutts, A. Ferapontov, A. Garabedian, J. Hakala, U. Heintz, O. Jesus, E. Laird, G. Landsberg, Z. Mao, M. Narain, S. Piperov, S. Sagir, R. Syarif

**University of California, Davis, Davis, USA**
R. Breedon, G. Breto, M. Calderon De La Barca Sanchez, S. Chauhan, M. Chertok, J. Conway, R. Conway, P.T. Cox, R. Erbacher, G. Funk, M. Gardner, W. Ko, R. Lander, C. Mclean, M. Mulhearn, D. Pellett, J. Pilot, F. Ricci-Tam, S. Shalhout, J. Smith, M. Squires, D. Stolp, M. Tripathi, S. Wilbur, R. Yohay

**University of California, Los Angeles, USA**
R. Cousins, P. Everaerts, A. Florent, J. Hauser, M. Ignatenko, D. Saltzberg, E. Takasugi, V. Valuev, M. Weber

**University of California, Riverside, Riverside, USA**
K. Burt, R. Clare, J. Ellison, J.W. Gary, G. Hanson, J. Heilman, M. Ivova PANEVA, P. Jandir, E. Kennedy, F. Lacroix, O.R. Long, M. Malberti, M. Olmedo Negrete, A. Shrinivas, H. Wei, S. Wimpenny, B. R. Yates

**University of California, San Diego, La Jolla, USA**
J.G. Branson, G.B. Cerati, S. Cittolin, R.T. D'Agnolo, M. Derdzinski, A. Holzner, R. Kelley, D. Klein, J. Letts, I. Macneill, D. Olivito, S. Padhi, M. Pieri, M. Sani, V. Sharma, S. Simon, M. Tadel, A. Vartak, S. Wasserbaech[66], C. Welke, F. Würthwein, A. Yagil, G. Zevi Della Porta

**University of California, Santa Barbara, Santa Barbara, USA**
J. Bradmiller-Feld, C. Campagnari, A. Dishaw, V. Dutta, K. Flowers, M. Franco Sevilla, P. Geffert, C. George, F. Golf, L. Gouskos, J. Gran, J. Incandela, N. Mccoll, S.D. Mullin, J. Richman, D. Stuart, I. Suarez, C. West, J. Yoo

**California Institute of Technology, Pasadena, USA**
D. Anderson, A. Apresyan, J. Bendavid, A. Bornheim, J. Bunn, Y. Chen, J. Duarte, A. Mott, H.B. Newman, C. Pena, M. Spiropulu, J.R. Vlimant, S. Xie, R.Y. Zhu

**Carnegie Mellon University, Pittsburgh, USA**
M.B. Andrews, V. Azzolini, A. Calamba, B. Carlson, T. Ferguson, M. Paulini, J. Russ, M. Sun, H. Vogel, I. Vorobiev

**University of Colorado Boulder, Boulder, USA**
J.P. Cumalat, W.T. Ford, A. Gaz, F. Jensen, A. Johnson, M. Krohn, T. Mulholland, U. Nauenberg, K. Stenson, S.R. Wagner

**Cornell University, Ithaca, USA**
J. Alexander, A. Chatterjee, J. Chaves, J. Chu, S. Dittmer, N. Eggert, N. Mirman, G. Nicolas Kaufman, J.R. Patterson, A. Rinkevicius, A. Ryd, L. Skinnari, L. Soffi, W. Sun, S.M. Tan, W.D. Teo, J. Thom, J. Thompson, J. Tucker, Y. Weng, P. Wittich

**Fermi National Accelerator Laboratory, Batavia, USA**
S. Abdullin, M. Albrow, G. Apollinari, S. Banerjee, L.A.T. Bauerdick, A. Beretvas, J. Berryhill, P.C. Bhat, G. Bolla, K. Burkett, J.N. Butler, H.W.K. Cheung, F. Chlebana, S. Cihangir, V.D. Elvira, I. Fisk, J. Freeman, E. Gottschalk, L. Gray, D. Green, S. Grünendahl, O. Gutsche, J. Hanlon, D. Hare, R.M. Harris, S. Hasegawa, J. Hirschauer, Z. Hu, B. Jayatilaka, S. Jindariani, M. Johnson, U. Joshi, B. Klima, B. Kreis, S. Lammel, J. Lewis, J. Linacre, D. Lincoln, R. Lipton, T. Liu, R. Lopes De Sá, J. Lykken, K. Maeshima, J.M. Marraffino, S. Maruyama, D. Mason, P. McBride, P. Merkel, S. Mrenna, S. Nahn, C. Newman-Holmes[†], V. O'Dell, K. Pedro, O. Prokofyev,

G. Rakness, E. Sexton-Kennedy, A. Soha, W.J. Spalding, L. Spiegel, S. Stoynev, N. Strobbe, L. Taylor, S. Tkaczyk, N.V. Tran, L. Uplegger, E.W. Vaandering, C. Vernieri, M. Verzocchi, R. Vidal, M. Wang, H.A. Weber, A. Whitbeck

**University of Florida, Gainesville, USA**
D. Acosta, P. Avery, P. Bortignon, D. Bourilkov, A. Brinkerhoff, A. Carnes, M. Carver, D. Curry, S. Das, R.D. Field, I.K. Furic, J. Konigsberg, A. Korytov, K. Kotov, P. Ma, K. Matchev, H. Mei, P. Milenovic[67], G. Mitselmakher, D. Rank, R. Rossin, L. Shchutska, M. Snowball, D. Sperka, N. Terentyev, L. Thomas, J. Wang, S. Wang, J. Yelton

**Florida International University, Miami, USA**
S. Linn, P. Markowitz, G. Martinez, J.L. Rodriguez

**Florida State University, Tallahassee, USA**
A. Ackert, J.R. Adams, T. Adams, A. Askew, S. Bein, J. Bochenek, B. Diamond, J. Haas, S. Hagopian, V. Hagopian, K.F. Johnson, A. Khatiwada, H. Prosper, M. Weinberg

**Florida Institute of Technology, Melbourne, USA**
M.M. Baarmand, V. Bhopatkar, S. Colafranceschi[68], M. Hohlmann, H. Kalakhety, D. Noonan, T. Roy, F. Yumiceva

**University of Illinois at Chicago (UIC), Chicago, USA**
M.R. Adams, L. Apanasevich, D. Berry, R.R. Betts, I. Bucinskaite, R. Cavanaugh, O. Evdokimov, L. Gauthier, C.E. Gerber, D.J. Hofman, P. Kurt, C. O'Brien, I.D. Sandoval Gonzalez, P. Turner, N. Varelas, Z. Wu, M. Zakaria, J. Zhang

**The University of Iowa, Iowa City, USA**
B. Bilki[69], W. Clarida, K. Dilsiz, S. Durgut, R.P. Gandrajula, M. Haytmyradov, V. Khristenko, J.-P. Merlo, H. Mermerkaya[70], A. Mestvirishvili, A. Moeller, J. Nachtman, H. Ogul, Y. Onel, F. Ozok[71], A. Penzo, C. Snyder, E. Tiras, J. Wetzel, K. Yi

**Johns Hopkins University, Baltimore, USA**
I. Anderson, B.A. Barnett, B. Blumenfeld, A. Cocoros, N. Eminizer, D. Fehling, L. Feng, A.V. Gritsan, P. Maksimovic, M. Osherson, J. Roskes, U. Sarica, M. Swartz, M. Xiao, Y. Xin, C. You

**The University of Kansas, Lawrence, USA**
P. Baringer, A. Bean, C. Bruner, J. Castle, R.P. Kenny III, A. Kropivnitskaya, D. Majumder, M. Malek, W. Mcbrayer, M. Murray, S. Sanders, R. Stringer, Q. Wang

**Kansas State University, Manhattan, USA**
A. Ivanov, K. Kaadze, S. Khalil, M. Makouski, Y. Maravin, A. Mohammadi, L.K. Saini, N. Skhirtladze, S. Toda

**Lawrence Livermore National Laboratory, Livermore, USA**
D. Lange, F. Rebassoo, D. Wright

**University of Maryland, College Park, USA**
C. Anelli, A. Baden, O. Baron, A. Belloni, B. Calvert, S.C. Eno, C. Ferraioli, J.A. Gomez, N.J. Hadley, S. Jabeen, R.G. Kellogg, T. Kolberg, J. Kunkle, Y. Lu, A.C. Mignerey, Y.H. Shin, A. Skuja, M.B. Tonjes, S.C. Tonwar

**Massachusetts Institute of Technology, Cambridge, USA**
A. Apyan, R. Barbieri, A. Baty, R. Bi, K. Bierwagen, S. Brandt, W. Busza, I.A. Cali, Z. Demiragli, L. Di Matteo, G. Gomez Ceballos, M. Goncharov, D. Gulhan, Y. Iiyama, G.M. Innocenti,

M. Klute, D. Kovalskyi, K. Krajczar, Y.S. Lai, Y.-J. Lee, A. Levin, P.D. Luckey, A.C. Marini, C. Mcginn, C. Mironov, S. Narayanan, X. Niu, C. Paus, C. Roland, G. Roland, J. Salfeld-Nebgen, G.S.F. Stephans, K. Sumorok, K. Tatar, M. Varma, D. Velicanu, J. Veverka, J. Wang, T.W. Wang, B. Wyslouch, M. Yang, V. Zhukova

**University of Minnesota, Minneapolis, USA**
A.C. Benvenuti, B. Dahmes, A. Evans, A. Finkel, A. Gude, P. Hansen, S. Kalafut, S.C. Kao, K. Klapoetke, Y. Kubota, Z. Lesko, J. Mans, S. Nourbakhsh, N. Ruckstuhl, R. Rusack, N. Tambe, J. Turkewitz

**University of Mississippi, Oxford, USA**
J.G. Acosta, S. Oliveros

**University of Nebraska-Lincoln, Lincoln, USA**
E. Avdeeva, R. Bartek, K. Bloom, S. Bose, D.R. Claes, A. Dominguez, C. Fangmeier, R. Gonzalez Suarez, R. Kamalieddin, D. Knowlton, I. Kravchenko, F. Meier, J. Monroy, F. Ratnikov, J.E. Siado, G.R. Snow, B. Stieger

**State University of New York at Buffalo, Buffalo, USA**
M. Alyari, J. Dolen, J. George, A. Godshalk, C. Harrington, I. Iashvili, J. Kaisen, A. Kharchilava, A. Kumar, A. Parker, S. Rappoccio, B. Roozbahani

**Northeastern University, Boston, USA**
G. Alverson, E. Barberis, D. Baumgartel, M. Chasco, A. Hortiangtham, A. Massironi, D.M. Morse, D. Nash, T. Orimoto, R. Teixeira De Lima, D. Trocino, R.-J. Wang, D. Wood, J. Zhang

**Northwestern University, Evanston, USA**
S. Bhattacharya, K.A. Hahn, A. Kubik, J.F. Low, N. Mucia, N. Odell, B. Pollack, M.H. Schmitt, K. Sung, M. Trovato, M. Velasco

**University of Notre Dame, Notre Dame, USA**
N. Dev, M. Hildreth, C. Jessop, D.J. Karmgard, N. Kellams, K. Lannon, N. Marinelli, F. Meng, C. Mueller, Y. Musienko[38], M. Planer, A. Reinsvold, R. Ruchti, N. Rupprecht, G. Smith, S. Taroni, N. Valls, M. Wayne, M. Wolf, A. Woodard

**The Ohio State University, Columbus, USA**
L. Antonelli, J. Brinson, B. Bylsma, L.S. Durkin, S. Flowers, A. Hart, C. Hill, R. Hughes, W. Ji, T.Y. Ling, B. Liu, W. Luo, D. Puigh, M. Rodenburg, B.L. Winer, H.W. Wulsin

**Princeton University, Princeton, USA**
O. Driga, P. Elmer, J. Hardenbrook, P. Hebda, S.A. Koay, P. Lujan, D. Marlow, T. Medvedeva, M. Mooney, J. Olsen, C. Palmer, P. Piroué, D. Stickland, C. Tully, A. Zuranski

**University of Puerto Rico, Mayaguez, USA**
S. Malik

**Purdue University, West Lafayette, USA**
A. Barker, V.E. Barnes, D. Benedetti, D. Bortoletto, L. Gutay, M.K. Jha, M. Jones, A.W. Jung, K. Jung, D.H. Miller, N. Neumeister, B.C. Radburn-Smith, X. Shi, I. Shipsey, D. Silvers, J. Sun, A. Svyatkovskiy, F. Wang, W. Xie, L. Xu

**Purdue University Calumet, Hammond, USA**
N. Parashar, J. Stupak

**Rice University, Houston, USA**
A. Adair, B. Akgun, Z. Chen, K.M. Ecklund, F.J.M. Geurts, M. Guilbaud, W. Li, B. Michlin, M. Northup, B.P. Padley, R. Redjimi, J. Roberts, J. Rorie, Z. Tu, J. Zabel

**University of Rochester, Rochester, USA**
B. Betchart, A. Bodek, P. de Barbaro, R. Demina, Y. Eshaq, T. Ferbel, M. Galanti, A. Garcia-Bellido, J. Han, O. Hindrichs, A. Khukhunaishvili, K.H. Lo, P. Tan, M. Verzetti

**Rutgers, The State University of New Jersey, Piscataway, USA**
J.P. Chou, E. Contreras-Campana, D. Ferencek, Y. Gershtein, E. Halkiadakis, M. Heindl, D. Hidas, E. Hughes, S. Kaplan, R. Kunnawalkam Elayavalli, A. Lath, K. Nash, H. Saka, S. Salur, S. Schnetzer, D. Sheffield, S. Somalwar, R. Stone, S. Thomas, P. Thomassen, M. Walker

**University of Tennessee, Knoxville, USA**
M. Foerster, J. Heideman, G. Riley, K. Rose, S. Spanier, K. Thapa

**Texas A&M University, College Station, USA**
O. Bouhali[72], A. Castaneda Hernandez[72], A. Celik, M. Dalchenko, M. De Mattia, A. Delgado, S. Dildick, R. Eusebi, J. Gilmore, T. Huang, T. Kamon[73], V. Krutelyov, R. Mueller, I. Osipenkov, Y. Pakhotin, R. Patel, A. Perloff, L. Perniè, D. Rathjens, A. Rose, A. Safonov, A. Tatarinov, K.A. Ulmer

**Texas Tech University, Lubbock, USA**
N. Akchurin, C. Cowden, J. Damgov, C. Dragoiu, P.R. Dudero, J. Faulkner, S. Kunori, K. Lamichhane, S.W. Lee, T. Libeiro, S. Undleeb, I. Volobouev, Z. Wang

**Vanderbilt University, Nashville, USA**
E. Appelt, A.G. Delannoy, S. Greene, A. Gurrola, R. Janjam, W. Johns, C. Maguire, Y. Mao, A. Melo, H. Ni, P. Sheldon, S. Tuo, J. Velkovska, Q. Xu

**University of Virginia, Charlottesville, USA**
M.W. Arenton, P. Barria, B. Cox, B. Francis, J. Goodell, R. Hirosky, A. Ledovskoy, H. Li, C. Neu, T. Sinthuprasith, X. Sun, Y. Wang, E. Wolfe, J. Wood, F. Xia

**Wayne State University, Detroit, USA**
C. Clarke, R. Harr, P.E. Karchin, C. Kottachchi Kankanamge Don, P. Lamichhane, J. Sturdy

**University of Wisconsin - Madison, Madison, WI, USA**
D.A. Belknap, D. Carlsmith, S. Dasu, L. Dodd, S. Duric, B. Gomber, M. Grothe, M. Herndon, A. Hervé, P. Klabbers, A. Lanaro, A. Levine, K. Long, R. Loveless, A. Mohapatra, I. Ojalvo, T. Perry, G.A. Pierro, G. Polese, T. Ruggles, T. Sarangi, A. Savin, A. Sharma, N. Smith, W.H. Smith, D. Taylor, P. Verwilligen, N. Woods

†: Deceased
1: Also at Vienna University of Technology, Vienna, Austria
2: Also at State Key Laboratory of Nuclear Physics and Technology, Peking University, Beijing, China
3: Also at Institut Pluridisciplinaire Hubert Curien, Université de Strasbourg, Université de Haute Alsace Mulhouse, CNRS/IN2P3, Strasbourg, France
4: Also at Universidade Estadual de Campinas, Campinas, Brazil
5: Also at Centre National de la Recherche Scientifique (CNRS) - IN2P3, Paris, France
6: Also at Université Libre de Bruxelles, Bruxelles, Belgium
7: Also at Laboratoire Leprince-Ringuet, Ecole Polytechnique, IN2P3-CNRS, Palaiseau, France
8: Also at Joint Institute for Nuclear Research, Dubna, Russia

9: Also at Helwan University, Cairo, Egypt
10: Now at Zewail City of Science and Technology, Zewail, Egypt
11: Also at Ain Shams University, Cairo, Egypt
12: Also at Fayoum University, El-Fayoum, Egypt
13: Now at British University in Egypt, Cairo, Egypt
14: Also at Université de Haute Alsace, Mulhouse, France
15: Also at CERN, European Organization for Nuclear Research, Geneva, Switzerland
16: Also at Skobeltsyn Institute of Nuclear Physics, Lomonosov Moscow State University, Moscow, Russia
17: Also at Tbilisi State University, Tbilisi, Georgia
18: Also at RWTH Aachen University, III. Physikalisches Institut A, Aachen, Germany
19: Also at University of Hamburg, Hamburg, Germany
20: Also at Brandenburg University of Technology, Cottbus, Germany
21: Also at Institute of Nuclear Research ATOMKI, Debrecen, Hungary
22: Also at MTA-ELTE Lendület CMS Particle and Nuclear Physics Group, Eötvös Loránd University, Budapest, Hungary
23: Also at University of Debrecen, Debrecen, Hungary
24: Also at Indian Institute of Science Education and Research, Bhopal, India
25: Also at University of Visva-Bharati, Santiniketan, India
26: Now at King Abdulaziz University, Jeddah, Saudi Arabia
27: Also at University of Ruhuna, Matara, Sri Lanka
28: Also at Isfahan University of Technology, Isfahan, Iran
29: Also at University of Tehran, Department of Engineering Science, Tehran, Iran
30: Also at Plasma Physics Research Center, Science and Research Branch, Islamic Azad University, Tehran, Iran
31: Also at Università degli Studi di Siena, Siena, Italy
32: Also at Purdue University, West Lafayette, USA
33: Now at Hanyang University, Seoul, Korea
34: Also at International Islamic University of Malaysia, Kuala Lumpur, Malaysia
35: Also at Malaysian Nuclear Agency, MOSTI, Kajang, Malaysia
36: Also at Consejo Nacional de Ciencia y Tecnología, Mexico city, Mexico
37: Also at Warsaw University of Technology, Institute of Electronic Systems, Warsaw, Poland
38: Also at Institute for Nuclear Research, Moscow, Russia
39: Now at National Research Nuclear University 'Moscow Engineering Physics Institute' (MEPhI), Moscow, Russia
40: Also at St. Petersburg State Polytechnical University, St. Petersburg, Russia
41: Also at University of Florida, Gainesville, USA
42: Also at California Institute of Technology, Pasadena, USA
43: Also at Faculty of Physics, University of Belgrade, Belgrade, Serbia
44: Also at INFN Sezione di Roma; Università di Roma, Roma, Italy
45: Also at National Technical University of Athens, Athens, Greece
46: Also at Scuola Normale e Sezione dell'INFN, Pisa, Italy
47: Also at National and Kapodistrian University of Athens, Athens, Greece
48: Also at Riga Technical University, Riga, Latvia
49: Also at Institute for Theoretical and Experimental Physics, Moscow, Russia
50: Also at Albert Einstein Center for Fundamental Physics, Bern, Switzerland
51: Also at Adiyaman University, Adiyaman, Turkey
52: Also at Mersin University, Mersin, Turkey
53: Also at Cag University, Mersin, Turkey

54: Also at Piri Reis University, Istanbul, Turkey
55: Also at Gaziosmanpasa University, Tokat, Turkey
56: Also at Ozyegin University, Istanbul, Turkey
57: Also at Izmir Institute of Technology, Izmir, Turkey
58: Also at Marmara University, Istanbul, Turkey
59: Also at Kafkas University, Kars, Turkey
60: Also at Istanbul Bilgi University, Istanbul, Turkey
61: Also at Yildiz Technical University, Istanbul, Turkey
62: Also at Hacettepe University, Ankara, Turkey
63: Also at Rutherford Appleton Laboratory, Didcot, United Kingdom
64: Also at School of Physics and Astronomy, University of Southampton, Southampton, United Kingdom
65: Also at Instituto de Astrofísica de Canarias, La Laguna, Spain
66: Also at Utah Valley University, Orem, USA
67: Also at University of Belgrade, Faculty of Physics and Vinca Institute of Nuclear Sciences, Belgrade, Serbia
68: Also at Facoltà Ingegneria, Università di Roma, Roma, Italy
69: Also at Argonne National Laboratory, Argonne, USA
70: Also at Erzincan University, Erzincan, Turkey
71: Also at Mimar Sinan University, Istanbul, Istanbul, Turkey
72: Also at Texas A&M University at Qatar, Doha, Qatar
73: Also at Kyungpook National University, Daegu, Korea